The Space-Based Visible Program

Grant H. Stokes, Curt von Braun, Ramaswamy Sridharan, David Harrison, and Jayant Sharma

The Midcourse Space Experiment satellite was launched in 1996 into an 898-km altitude, near sun-synchronous orbit. A principal sensor on board the satellite is the Space-Based Visible (SBV) sensor, a visible-band electro-optical camera designed at Lincoln Laboratory to perform the first technical and functional demonstration of space-based space surveillance. The principal task of the SBV sensor is to gather metric and photometric information on a variety of resident space objects (RSO). In 1997, after the successful technology-demonstration phase of the mission, the SBV sensor was transitioned to a Contributing Sensor in the Space-Surveillance Network. Since April 1998, upon completion of the transition and testing phase, the SBV sensor has responded to daily tasking requests from the 1st Command and Control Squadron, in Cheyenne Mountain, in support of routine RSO catalog maintenance. The Space-Based Space-Surveillance Operations, funded through an Advanced Concept Technology Demonstration with the Office of the Secretary of Defense, the Ballistic Missile Defense Organization, and Air Force Space Command, is now providing the Space-Surveillance Network with the first operational space-based space-surveillance sensor. With its orbital location, wide field of view, and high metric accuracy, the SBV sensor has made a significant contribution to the Space-Surveillance Network, providing more tracks of objects in the geosynchronous belt than any other Space-Surveillance Network sensor.

The field of space surveillance was ushered in with the launch of Sputnik I in 1957. Since that time, Lincoln Laboratory has been deeply involved in the development of radar and optical technology in support of space surveillance. Much of the technology behind today's deep-space surveillance radars and the ground-based electro-optical deep-space surveillance (GEODSS) cameras was developed from Lincoln Laboratory prototype systems.

In the four decades since the launch of Sputnik, the technology supporting the mission of space surveillance has developed and matured considerably. Today an elaborate data-analysis system with conventions, procedures, communications, and practices has evolved. The system has expanded from that of low-altitude surveillance—tracking satellites that range in altitude from a few hundred to several thousand kilometers—to deep-space surveillance, tracking objects that are far beyond the 36,000-km altitude of the geosynchronous belt. Currently, the resident space object (RSO) catalog contains more than 8000 entries, consisting of active and inactive satellites, rocket bodies, and debris, with an active subset of over 800 objects.

Capabilities exist today to measure positions of low-earth-orbit objects with sizes as small as a few tens of centimeters, and geosynchronous-orbit objects with sizes on the order of a meter. The deep-space radars at Lincoln Laboratory's Millstone Hill in Westford, Massachusetts, and on the Kwajalein atoll in the Pacific Ocean are able to track geosynchronous satellites with an accuracy of a few meters. These results clearly indicate the considerable progress made in the past forty years. We are on the verge, however, of the next major technological change in space surveillance, namely, space-based space surveillance.

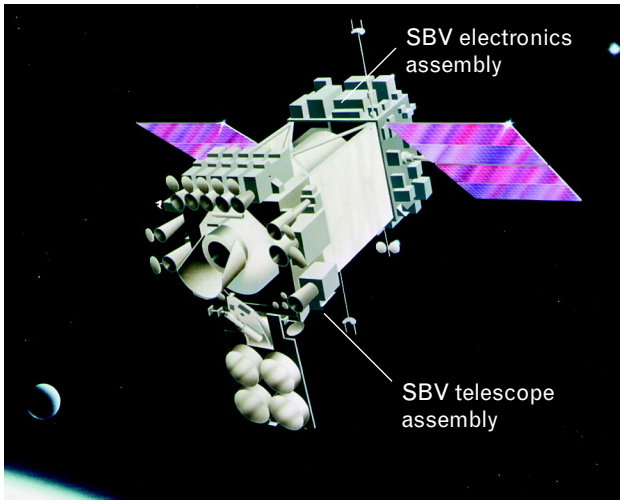

FIGURE 1. The Space-Based Visible (SBV) sensor on the Midcourse Space Experiment (MSX) satellite. The MSX satellite was designed and integrated at the Applied Physics Laboratory (APL) at Johns Hopkins University. The SBV sensor, which was designed and integrated at Lincoln Laboratory, is the first space-based space-surveillance sensor.

Overview of the Space-Based Visible Program

Since April 1996 the Space-Based Visible (SBV) sensor on the Midcourse Space Experiment (MSX) satellite, illustrated in Figure 1, has been gathering data as part of a technology demonstration of space-based space surveillance. The first eighteen months on orbit were dedicated to validating the concept of space-based space surveillance and assessing the performance of the SBV sensor. During this period the Space-Surveillance Principal Investigator team conducted a variety of experiments. These experiments demonstrated that (1) space-based space surveillance was not only possible but highly productive, and (2) the SBV sensor could serve as an operational asset to the Space-Surveillance Network [1]. On this basis, commencing in October 1997, the SBV sensor was transitioned from an experimental sensor to a Contributing Sensor within the Space-Surveillance Network. This transition occurred as part of an Advanced Concept Technology Demonstration (ACTD) sponsored by the Office of the Secretary of Defense, the Ballistic Missile Defense Organization (BMDO), and Air Force Space Command (which has the responsibility of keeping a current catalog of RSOs orbiting the earth). This technology demonstration supplied Air Force Space Command with the first space-based space-surveillance observations, starting on a trial basis in April 1998 and becoming fully operational in May 1998.

The SBV program has a number of general objectives that were established in the late 1980s during the early design phase [2]. Since the inception of the space-based space-surveillance operations ACTD in late 1997, specific objectives were added to address needs within the Space-Surveillance Network. The principal objectives are as follows.

Technology Demonstrations. The SBV sensor is a space-based technology demonstration program for three major new technologies: (1) high off-axis rejection optics to allow detection of faint targets near the sunlit earth limb; (2) advanced staring focal-plane arrays to allow for sensitive searches of large areas of the sky; and (3) an onboard signal processing capability to reduce the large volume of focal-plane data to a manageable set of data on stars and targets.

Space-Surveillance Demonstrations. The SBV sensor was designed primarily to demonstrate the concept of space-based space surveillance. The objectives to address this task include (1) assessment of SBV metric performance in support of space surveillance, (2) performance of routine space-surveillance operations such as timely and productive response to standard Air Force Space Command tasking and wide-area search, and (3) acquisition of raw full-frame background and phenomenological data for future advanced signal processor development.

Ballistic Missile Data Acquisition. One objective of the SBV program was to gather phenomenology data on a broad range of missiles and other targets during dedicated and cooperative BMDO tests. In addition, other MSX principal investigators used the SBV sensor to collect broadband visible wavelength data on a variety of earth-limb and celestial backgrounds [3].

ACTD Operations as a Contributing Sensor. These recent objectives include (1) integration of the SBV sensor into the Space-Surveillance Network, which involves exercising the Space Defense Operations Center in Cheyenne Mountain, Colorado, with real space-based space-surveillance data; (2) operational demonstration of the fusion of SBV data with data from the ground-based network; (3) demonstration

of routine response to space-surveillance tasking from Space Command; and (4) performance of wide-area searches of the geosynchronous orbital belt.

The overall goal of the SBV program is to establish a legacy for future space-based space-surveillance systems and to facilitate in the transfer of technology to the eventual operational system. This article provides an introduction to the SBV sensor and the results achieved since the launch of the MSX satellite, both in the experimental demonstration phase of the program over the first eighteen months and in the ongoing operations as a Contributing Sensor to the Space-Surveillance Network.

Technology Demonstrations

The first eighteen months of operation of the SBV sensor were devoted to the experimental demonstration of the technologies and capabilities of the sensor for space-surveillance and ballistic-missile-defense missions. During this phase, a large volume of raw full-frame data, as well as signal-processed data, was collected, analyzed, and archived in the SBV Processing and Operations Control Center (SPOCC) at Lincoln Laboratory. The results of the key technology and space-surveillance demonstrations are described in this section.

As outlined in the previous section, a number of important technologies have been demonstrated with the SBV sensor since launch. Figure 2 shows the hardware associated with these technologies. The first important technology, the high stray-light rejection design of the SBV telescope, allows for the detection of faint targets in high background environments near the sunlit earth limb. This characteristic is essential for the collection of phenomenology data on missile targets as well as on low-altitude RSOs. To accomplish this objective, the SBV employs an off-axis optical design, which gives the sensor its boxy structure, as shown in Figure 2(a). To aid in accomplishing this objective, the telescope and the mirrors were kept extremely clean during integration, launch, and operations, and they continue to remain clean to the present day. Scattered light can be maintained at low levels by minimizing the contamination internal to the stray-light rejection sensor.

The degree to which stray light is rejected can be quantified by the minimum detectable object that can be seen in the presence of stressing backgrounds. At the SBV Critical Design Review, the goal was set to establish the capability of detecting a 68-cm-diameter specular sphere with a reflectivity of 0.8 at a range of three thousand kilometers at a tangent height of a hundred kilometers above the sunlit earth. The detection-sensitivity results shown in Figure 3 illustrate that this goal was substantially exceeded; minimum detection capability is currently equivalent to a 22-cm-diameter sphere under the conditions described above. Figure 3 also shows that performance of the sensor has not degraded since delivery of the telescope to Lincoln Laboratory [4, 5].

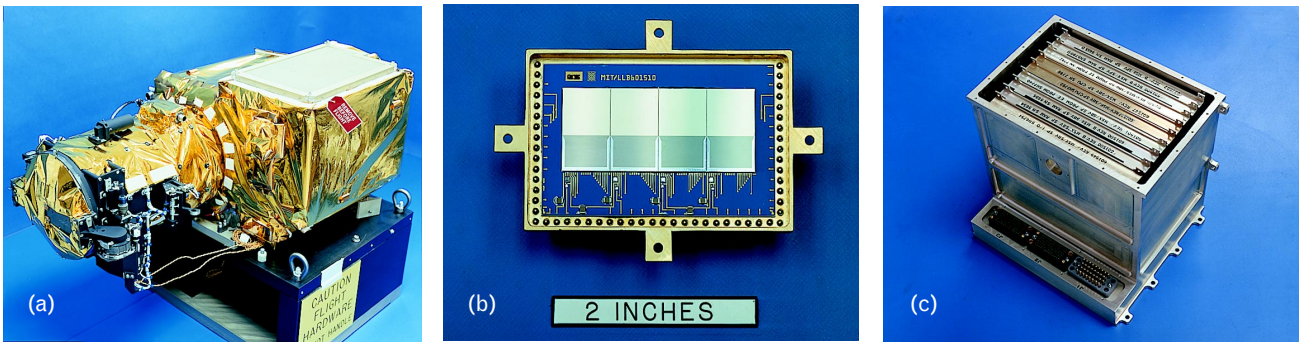

FIGURE 2. Major technology demonstrations on the SBV sensor include (a) high stray-light rejection optics, (b) the focal-plane array, and (c) the onboard signal processor. The high stray-light rejection capability allows the SBV sensor to track satellites near the sunlit earth limb. The four 420 × 422-pixel charge-coupled-devices (CCD) in the focal-plane array were fabricated in the Solid State division at Lincoln Laboratory in the late 1980s, and are used by the SBV sensor to detect photons from stars, satellites, and man-made debris. The onboard signal processor processes the focal-plane images to yield star and streak reports needed for routine space surveillance of resident space objects (RSO).

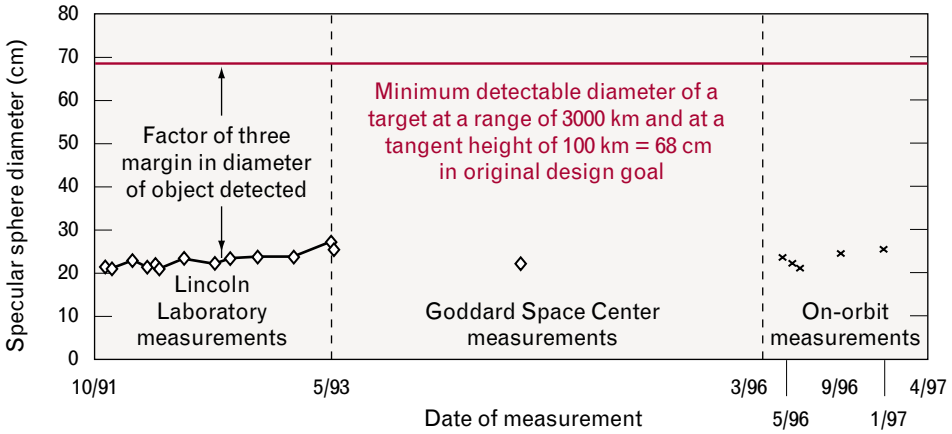

FIGURE 3. SBV detection sensitivity for space-borne targets. The on-orbit performance of the SBV sensor allows a 22-cm-diameter specular sphere (with a reflectivity of 0.8) to be tracked at a range of three thousand kilometers against an earth-limb background at a tangent height of one hundred kilometers. This capability exceeds the minimum detectable target diameter of 68 cm in the original design goal by a factor of three.

The second important technology incorporated into the design of the SBV sensor is low-noise charge-coupled-device (CCD) focal-plane arrays, shown in Figure 2(b). These four abutting 420 × 422-pixel arrays, each with a frame-store region for rapid readout, were designed and fabricated by the Semiconductor division at Lincoln Laboratory in the late 1980s.

CCD focal planes can be characterized by the dark current and its nonuniformity, along with the read noise, the charge-transfer efficiency, the well depth, and the percentage of damaged pixels. All of these are affected by on-orbit radiation. The SBV focal plane has exceeded performance expectations with respect to all these measures. The dark current and its nonuniformity appear to be increasing slowly because of radiation damage after almost three years in orbit. Even if the trend continues, however, the detection thresholds set at the SBV Critical Design Review will not be exceeded for another eight years. The focal-plane noise has also been affected slightly on orbit but will not be significant for more than ten years. There has also been no detectable change in the charge-transfer efficiency.

The third important technology demonstrated by the SBV program is that of the signal processor, shown in Figure 2(c). During routine space-surveillance operations, SBV sensor data are gathered by staring at a chosen location in the sky and collecting the image data over a sequence of frames, which is referred to as a frameset. A typical frameset includes as many as sixteen frames, resulting in almost three million pixels of information. The quantity of raw data generated by this process is far too large to be downloaded on the 1-Mbit/sec communications link periodically available to the MSX. The signal processor analyzes these three million pixels of information per field area and retains only the information most vital for space surveillance, thus reducing the data volume by as much as a factor of a thousand. The retained information consists of a selection of stars needed to determine the pointing of the SBV sensor and any streak signatures left by RSOs moving through the field of view. Figure 4 illustrates the effect of the signal processor by showing the superposition of sixteen raw frames (left) and the signal-processed image of these sixteen frames (right). In these images the stationary point sources are star detections and the streaks indicate detections of satellites [6–8].

The appendices entitled "Space-Based Visible Hardware" and "Calibration and Testing" provide a more detailed description of the SBV hardware—including the telescope, the focal-plane array, and the signal processor—and its construction, testing, and calibration.

In summary, the technology demonstrations on the SBV sensor have been extremely successful, paving the way for the design of future operational space-based space-surveillance systems.

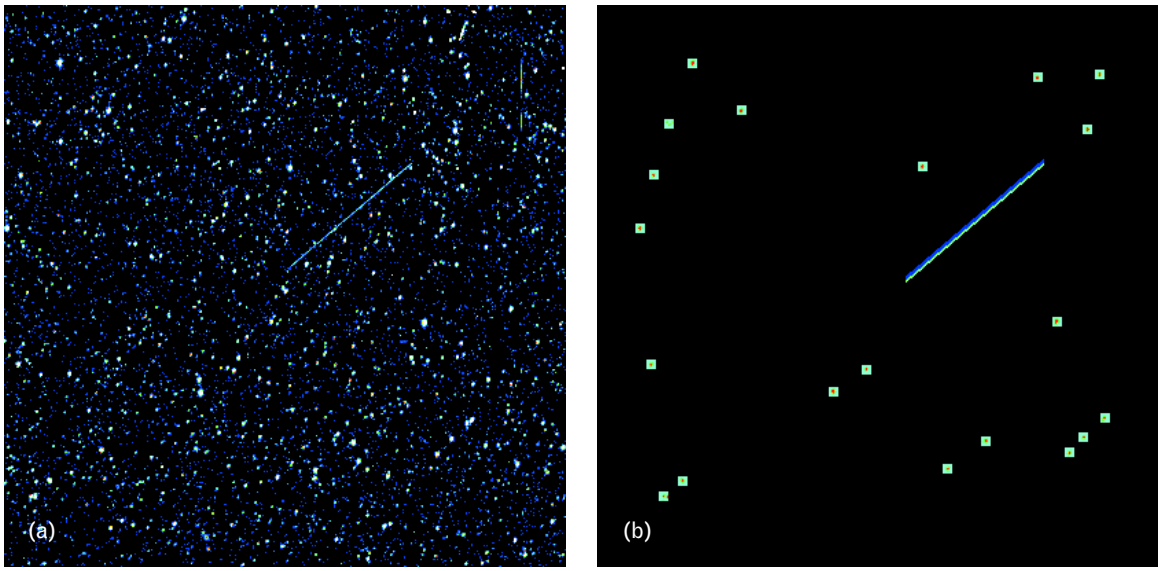

FIGURE 4. (a) SBV raw full-frame CCD exposure and (b) an associated signal processor image. The onboard signal processor reduces the volume of raw data by as much as a factor of a thousand, thus allowing for more effective downloading of image data across narrow-bandwidth telemetry links.

Space-Surveillance Demonstrations

In reference to the space-surveillance demonstrations outlined earlier, we now give a description of the metric and photometric accuracy of the SBV sensor, and its capabilities to perform wide-area search and geosynchronous-belt surveillance.

SBV Metric and Photometric Processing

Before we could assess the ability of the SBV sensor to conduct space-based space-surveillance activities, we had to determine both the metric and photometric characteristics of the sensor. The metric positioning of targets in the field of view of the SBV sensor requires knowledge of both the precise pointing of the sensor's boresight and the position of the SBV sensor on orbit at the time the data are gathered. By using the pointing information we can transform beginning and end points of the streaks detected on the focal plane, as shown in Figure 4, into two angular measurements on the sky, such as right ascension and declination. Each end point is considered to be a metric observation of the target. These observations can then be merged with other ground-based optical and radar observations on the same target in order to establish the target's trajectory.

The process of producing a metric observation involves several steps, as shown in the sequence of diagrams in Figure 5 [9]. With the SBV sensor in a staring mode tracking the stars, the raw sensor data are gathered on board by the CCD focal-plane array. The information contained in each raw frame is then passed to the signal processor, which extracts the pixel values and intensities associated with a preselected number of star detections. In addition, a moving-target-indicator algorithm within the signal processor identifies any objects moving relative to the stationary background. Pixel intensities and focal-plane coordinates for both the selected stars and the moving targets are downloaded in a signal processor report.

In the SPOCC, the star detections are centroided and the pattern and exact positions of detected stars are matched to a catalog of known stars. The differences between the detected positions and the catalog star positions are known as star-fit residuals. This process allows for a highly accurate determination of the pointing of the SBV sensor, without the use of additional sensors such as onboard gyroscopes. Through this technique, the pointing of the SBV sensor is routinely established to the level of a few tenths of an arcsecond. In addition, pointing is determined independently for each data acquisition, or look, which avoids common problems such as the drift and random walk typically associated with gyroscopes. Once

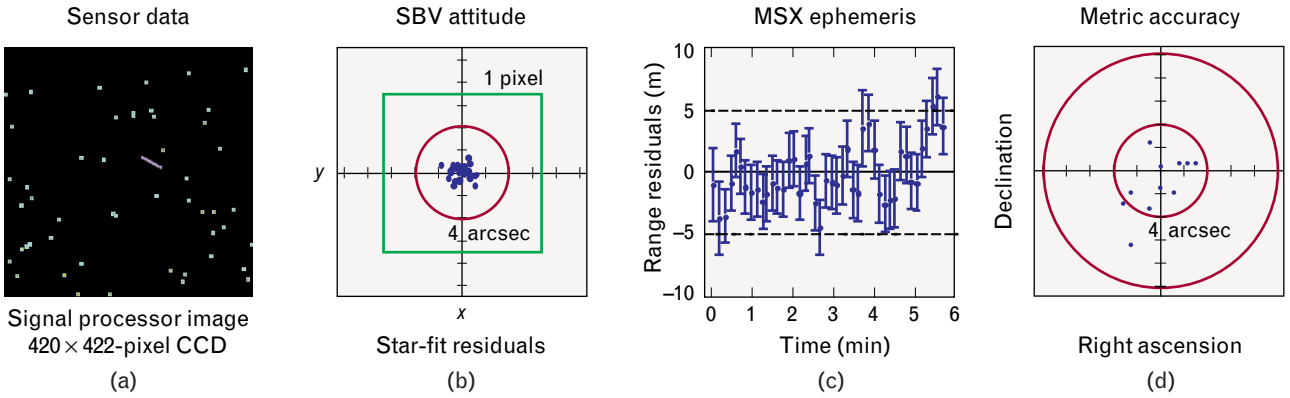

FIGURE 5. SBV metric data processing. Four necessary elements are required to produce angular measurements of a target's position on the sky. These elements are (a) the sensor data; (b) the SBV attitude, or boresight pointing; (c) the position, or ephemeris, of the MSX satellite at the time the target was viewed; and (d) the end points of the focal-plane streak left by the target. The metric accuracy of the SBV sensor exceeds that of the other sensors in the ground-based electro-optical deep-space surveillance (GEODSS) operational network by a factor of two and a half.

pointing is established, we use this information to map the end points of the streaks on the focal plane to absolute angular positions on the sky, thus producing an observation [10, 11].

While the process described above is sufficient to produce angular measurements on targets from a space-based sensor, it is insufficient for the complete incorporation of these data into a ground-based tracking network. To accomplish this integration of data we must be able to determine the position, or ephemeris, of the MSX at the time the data were gathered. As part of an independent processing pipeline, Lincoln Laboratory has maintained the ephemeris of the MSX to an accuracy of six meters, surpassing the original SBV Critical Design Review goal of fifteen meters. The determination of the ephemeris of the MSX is accomplished by processing S-band ranging data from the Space Ground Link System, a network of ground-based telemetry sensors used by the U.S. Air Force to track its space assets [12–14]. (A Global Positioning System [GPS] receiver was not integrated on the MSX because of weight constraints and because of the nascent state of the GPS constellation of satellites in the late 1980s.)

To assess the metric performance of the SBV sensor we conduct routine on-orbit metric calibration. This calibration is accomplished by observing satellites with well-established positions and comparing these known positions with SBV-sensor-observed positions. During the design phase of the SBV program, the goal of producing 4-arcsec (one standard deviation) metric observations of RSOs was set. This 4-arcsec error budget is comprised of a wide variety of error sources, ranging from the estimated position of the SBV sensor on orbit to systematic uncertainties within the established star catalogs [6, 7, 15]. The method by which the total observational error of the SBV sensor is determined is by comparing SBV-observed positions of GPS satellites with known positions of the same satellites. The ephemerides of GPS

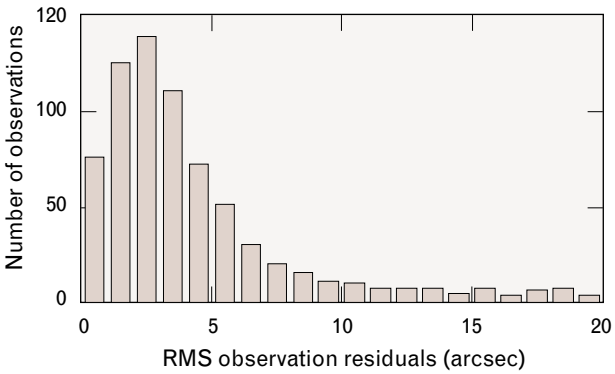

FIGURE 6. Residuals of SBV observations of GLONASS satellites. To perform on-orbit metric calibration, the SBV sensor routinely tracks Russian GLONASS and U.S. Global Positioning System (GPS) satellites. Because independent reference orbit positions for these satellites are well known, the measurement errors associated with the SBV sensor can be identified.

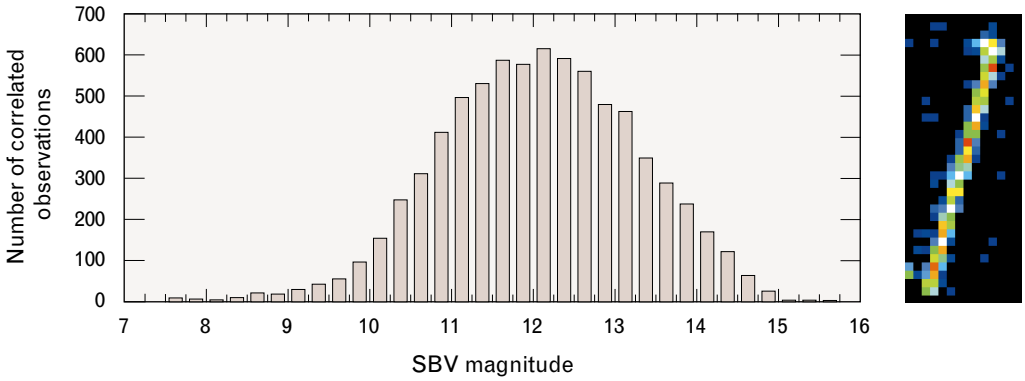

FIGURE 7. Histogram of the SBV detection brightness and a color intensity map of a detected RSO streak. An average brightness return from an RSO can be determined from the streak's signature. The brightness is quantified in terms of an SBV magnitude, which is similar to the visual magnitude used by astronomers to measure the brightness of stars. The difference between the two measurement systems is only about 0.1 to 0.2 magnitudes and exists because the SBV sensor is slightly more sensitive in the red.

satellites are determined by the Jet Propulsion Laboratory to better than fifty centimeters. Because of the high accuracy of these reference orbits, all differences in the comparison of the SBV observations with these accurately known orbital positions are attributable to the SBV sensor, with confirmation of the 4-arcsec metric accuracy shown in Figure 5(d). The inner circle of this diagram shows 4 arcsec; for comparison the outer circle of this diagram shows 10 arcsec, which is the design-specification accuracy requirement for the GEODSS[1] system. Figure 5(d) clearly shows that the SBV sensor improves metric accuracy by a factor of two and a half over the measurements of the GEODSS system.

Figure 6, which displays a large number of SBV observation residuals of GLONASS satellites, provides further validation of the metric performance of the SBV sensor. The GLONASS constellation of satellites represents the Russian equivalent of the U.S. GPS satellites, so independent orbital positions for its satellites are well determined. These results also show that the SBV sensor is routinely collecting metric data at the 4-arcsec accuracy level [16].

In addition to gathering metric observations of targets, the SBV sensor simultaneously acquires photometric observations. As mentioned earlier, intensity and pixel coordinates for streaks detected on RSOs are downloaded into the SPOCC as part of the routine telemetry data stream. The intensity information is used to determine an average brightness for the target during the time interval of data collection. The brightness of an object is quantified by the SBV magnitude, a logarithmic scale in which larger numbers represent fainter objects. Figure 7 shows an example of a detected signature, along with a histogram displaying months of photometric data collection as a function of brightness. This histogram indicates that the overall sensitivity of the SBV sensor is at 15th magnitude, with saturation occurring around 7th magnitude [16]. To date, a database of well over 100,000 observations on 2300 known objects has been established, and metric and photometric information is available on active payloads, inactive payloads, rocket bodies, upper stages, and debris.

Wide-Area-Search Capability of the SBV Sensor

The field of view of the SBV sensor is $1.4° \times 1.4°$ for each CCD. Because of the significant distortion inherent in the design of off-axis optical systems, the

[1] *The GEODSS system consists of nine one-meter-class telescopes, located at White Sands Missile Base, Socorro, New Mexico; on the island of Maui; and on the island of Diego Garcia in the Indian Ocean. The GEODSS system grew out of technology first developed at the Lincoln Laboratory Experimental Test Site in Socorro. In September 1998, the Space-Surveillance Network was augmented with the Transportable Optical System (TOS), another Lincoln Laboratory system fielded in southern Spain. All these systems contribute to deep-space surveillance.*

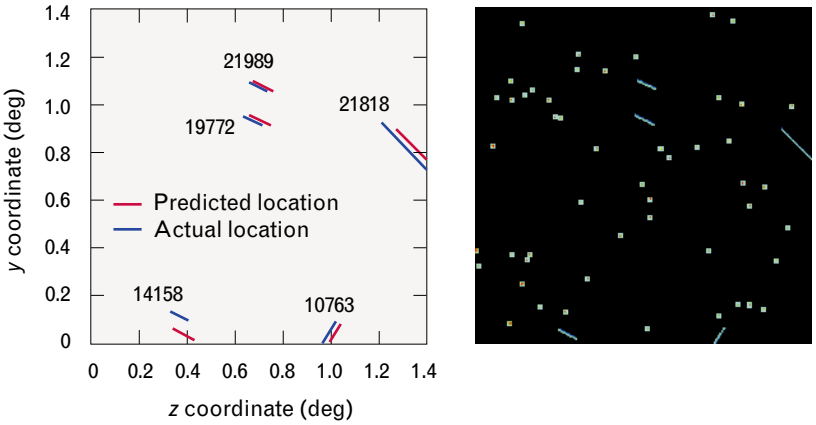

RSO	SBV–RSO range (km)	Description
10763	2794	NOAA 5 debris (LEO)
14158	41,247	Drifting Galaxy 1 (GEO)
19772	41,317	Intelsat V-F15 (GEO)
21818	11,260	Ariane Spelda debris (GEO transfer)
21989	41,334	Intelsat K (GEO)

FIGURE 8. Application of the wide field of view of the SBV sensor. With its 1.4°×1.4° field of view for each CCD, the SBV sensor is able to detect multiple objects per data collection. This figure, as an example, shows a data set containing objects in low earth orbit (LEO), geosynchronous earth orbit (GEO), and a GEO transfer orbit in the same look, as shown in the image on the right. This feature of the SBV sensor considerably aids in the sensor's productivity. The image on the left compares the SBV-detected positions with the predicted positions of those same targets in the RSO catalog.

total field of regard for all four CCDs is 6.6° × 1.4°. In comparison, the GEODSS telescopes have a circular field of view of 2° (the antiquated camera technology in the GEODSS telescopes actually limits the effective field of view considerably). Given that the signal processor can process only one CCD at a time, however, the instantaneous field of view of the SBV sensor is limited to that of one focal-plane array.

Figure 8 illustrates the capability of the wide field of view of the SBV sensor when it is applied to search applications. The data shown were gathered during a single look of the SBV sensor. The signatures of five correlated satellites are evident in the signal processor image on the right. The image on the left shows the detected streak data along with the predicted positions of those same targets, as based on the Space Command RSO catalog (detected stars have been omitted for clarity). While these five satellites are seen in the same field of view of the SBV sensor, they represent members of each of three orbital regimes—a geosynchronous earth orbit, a geosynchronous-earth-orbit transfer orbit, and a low earth orbit [17].

The wide-field-of-view search capabilities of the SBV sensor are highly useful in addressing the problem of "lost" objects. Objects can become lost from the RSO catalog if their predicted positions differ significantly from their actual positions. This problem can occur because an object has not been tracked for a long period of time or because the object has maneuvered. In either case, a space-surveillance sensor may be unsuccessful when attempting to acquire the object because the actual position of the object is outside the field of view of the sensor. With the narrow fields of view of ground-based deep-space radars and the GEODSS system, this problem can easily occur if an element set within the catalog has not been updated recently, or if the object has maneuvered.

Figure 9 illustrates this problem. For an object

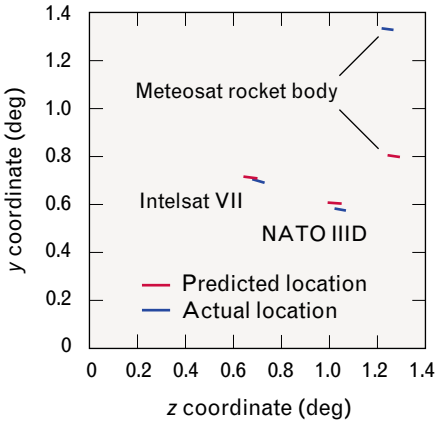

Satellite	Observed SBV magnitude	Age of element set (days)
Meteosat rocket body	14.5	38
NATO IIID	10.0	7
Intelsat VII	11.7	<1

FIGURE 9. The successful correlation of maneuvered or lost objects to the RSO catalog. Because the accuracy of the predicted position of an RSO in the catalog is strongly dependent upon how long ago the object was last tracked, the wide field of view of the SBV sensor is useful when looking for objects that have maneuvered or objects that have not been recently tracked, such as the Meteosat rocket body.

whose element set has been updated recently, such as the Intelsat VII satellite, the predicted position and the SBV-detected position are quite close. However, as the element sets of an object grow older, such as the NATO IIID satellite, deviations between the predicted position and the SBV-detected position begin to grow. In the case of the Meteosat rocket body, which has not been tracked in over a month, the predicted position and the actual position differ significantly. This object would not be seen by sensors with a field of view less than 0.5°. The wide field of view of the SBV sensor was able to detect and correlate the object successfully [16]. This capability has been exercised extensively during Contributing Sensor operations with Space Command; within the last eighteen months the SBV sensor has found fifty-five lost, maneuvered, and newly launched objects [18].

SBV Geosynchronous-Belt Surveillance

The SBV sensor has two capabilities that make it uniquely suited for surveillance of the geosynchronous belt. The first capability, as described earlier, is the wide field of view, allowing for multiple objects to be seen in one look. The other capability is that, being on orbit, the SBV sensor has access to all the RSOs in the entire geosynchronous belt, as illustrated in the upper part of Figure 10. In contrast, at least three ground-based sensors are required to achieve full coverage of this orbital regime. Further evidence of the capability of a space-based sensor to see the entire geosynchronous belt is shown in the lower part of Figure 10, which shows the actual positions of all the geostationary satellites observed by the SBV sensor during the eighteen months of the technology-demonstration phase [16].

Objects in geostationary orbits are exceedingly valuable to both military and commercial enterprises. Figure 11 shows one of the applications of the large

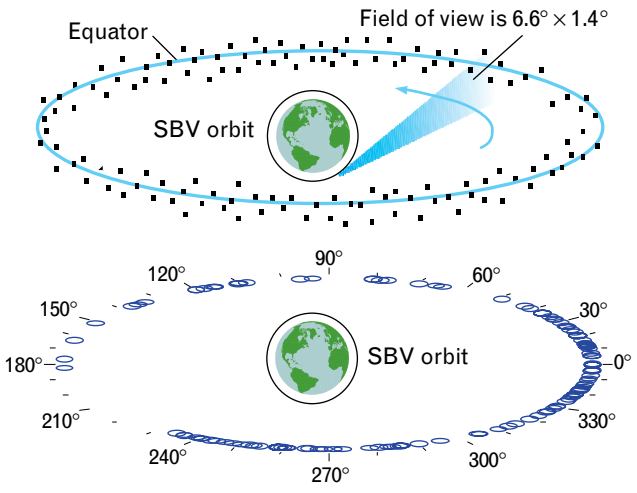

FIGURE 10. An illustration of geosynchronous-belt surveillance (top), and actual positions of all geosynchronous-belt satellites observed by the SBV sensor during the technology-demonstration phase of the program (bottom). Unlike ground-based sensors, the space-based SBV sensor has visual access to all of the RSOs in the geosynchronous belt.

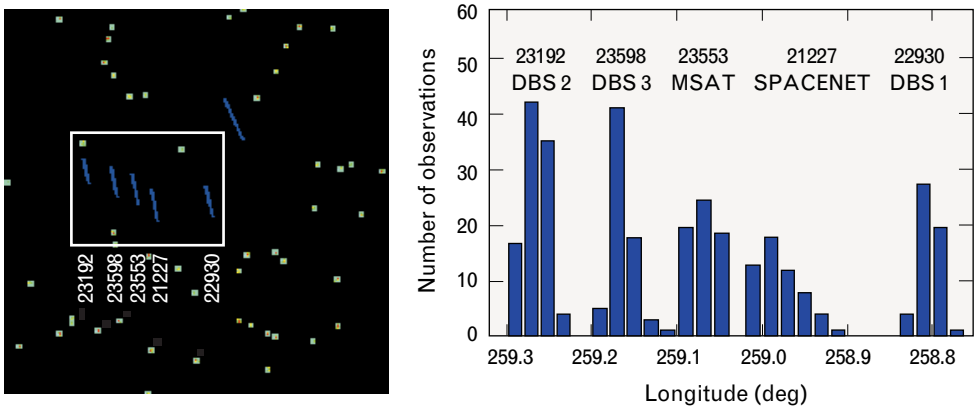

FIGURE 11. SBV observation of a cluster of five geosynchronous satellites. With its wide field of view and high-quality metric positioning of targets, the SBV sensor is able to see clusters in one data collection and contribute to the monitoring of these clusters. The satellites shown in this example are direct-broadcast satellites (DBS) and mobile-communications satellites (MSAT and SPACENET) situated over the equator, south of the continental United States. The histogram shows the total number of observations of these satellites as a function of longitude. The sixth streak in the frameset on the left is a Russian payload passing through the field of view of the SBV sensor.

field of view of the SBV sensor, in combination with its capability to survey the geosynchronous belt. The left side of Figure 11 shows a signal-processed frameset from the SBV sensor with detections on a cluster of five objects. Frequently, geosynchronous-belt satellites are maintained in clusters. Consortia of countries and commercial ventures are assigned longitude regions of the belt in which their satellites must remain. The cluster shown in Figure 11 consists of five direct-broadcast and mobile-telecommunications satellites located around 259° E longitude. The SBV sensor also detected one serendipitous object—a Russian payload—passing through the field of view.

The histogram on the right side of Figure 11 displays the total number of satellite observations as a function of longitude, indicating that these objects are maintained in close proximity to one another in their assigned locations. Since the SBV sensor can acquire data on the entire cluster at one time, the difficulty of properly correlating each member of the cluster to the RSO catalog is greatly eased. This issue of properly correlating members within a cluster is a significant problem for Space Command, a problem that the SBV sensor can aid in addressing. Images like those in Figure 11 show that a wide field-of-view, high-accuracy, space-based sensor can both support and enhance geosynchronous-belt surveillance [16].

SBV Data Catalog

In addition to routinely acquiring signal-processed observations in an operational capacity, the SBV sensor has been used to gather large quantities of raw full-frame data. Recall from the overview that these data are taken directly from the CCD, and thus contain the entire unreduced image. In this mode of collection, large quantities of data have been gathered over a wide variety of conditions. Highly stressing backgrounds, such as those taken near the sunlit earth limb and against the galactic plane, have been acquired and archived for use in developing the next generation of signal processing algorithms. In addition, sequences of framesets have been gathered in the high-radiation environment of the South Atlantic Anomaly (SAA), an area of higher than average densities of charged particles such as protons. These data provide insight into the operation of the signal processing algorithms in the presence of intense proton activity. The sidebar entitled "Radiation in Space" has a more thorough discussion of sensor data collection in a region of high radiation such as the SAA.

Phenomenology Data

In addition to its space-surveillance activities, the SBV sensor participated in a variety of target and

background phenomenology experiments that were conducted by other principal-investigator teams over the first year of the life of the MSX satellite. The key objectives associated with these activities were to assess the problems of detecting and tracking missiles against both sunlit and dark earth-limb backgrounds with a broadband visible wavelength sensor, and provide data for updating phenomenological models of the background. A large amount of data was collected, analyzed, and archived in the SPOCC, and some significant discoveries were made. These are reviewed in the sidebar entitled "Ballistic-Missile and Theater-Missile Data Collection."

SBV Operations as a Contributing Sensor

The success of the technology-demonstration phase of the SBV sensor led to interest on the part of Space Command into the use of the SBV as a Contributing Sensor to the Space-Surveillance Network for deep-space surveillance. This transition from an experimental sensor to an operational sensor was achieved by means of an ACTD program through joint funding from the Office of the Secretary of Defense, the BMDO, and Space Command. The transition began in October 1997 and was completed in May 1998.

The function of a Contributing Sensor to the Space-Surveillance Network, as with any member of the Network, is to gather observations on targets requested by the Air Force Space Command's 1st Command and Control Squadron (1CACS) in Cheyenne Mountain, near Colorado Springs, Colorado. Each day a tasking list of requests is sent to the SPOCC, and the SPOCC is expected to respond to the list within twenty-four hours. We now give a detailed discussion of daily operations of the SPOCC and the SBV sensor.

Contributing Sensor Concept of Operations

The problem of space surveillance is separated into two classes, that of low-altitude surveillance and that of deep-space surveillance. Low-altitude surveillance involves the acquisition, tracking, and cataloging of any RSO with a period of 225 minutes or less, while deep-space surveillance performs the same tasks for objects with periods greater than 225 minutes. The problem of acquiring and tracking an object in low altitude is addressed quite adequately with the use of phased-array radars, such as the FPS-85 radar located at Eglin Air Force Base in Florida. These radars are often operated in a fence configuration such that any object that is both large enough and within the range of the radar will be detected, and metric observations will be gathered. While these radars serve low-altitude surveillance well, they are not able to address the deep-space surveillance problem because of the large range to the targets. The network of ground sensors has limited capacity and coverage for deep-space tracking, and as a consequence a significant coverage gap exists in the eastern hemisphere of the geosynchronous belt. For these reasons, and because the space-based SBV sensor covers the entire geosynchronous belt, the SBV sensor was designed to focus on the problem of deep-space surveillance.

The operational philosophy of the SBV sensor, as described below, takes the characteristics of the sensor and the constraints of the MSX platform into account. Furthermore, the software that operates the SBV sensor, both on the ground and in space, optimizes the productivity of the system by exploiting the advantages while minimizing the impact of the constraints. This process occurs through ground operations with the SPOCC and at the Applied Physics Laboratory (APL) at Johns Hopkins University [19].

Figure 12 shows the ground network, which allows for communication between 1CACS at Cheyenne Mountain, 1st Space Operations Squadron (1SOPS) at Schriever Air Force Base outside Colorado Springs, Colorado, and the SPOCC at Lincoln Laboratory, and between the SPOCC, APL, and the MSX satellite. Currently, 1SOPS is responsible for coordinating and distributing all Air Force Satellite Control Network (AFSCN) downlink information, as well as serving as a backup to APL for MSX command and control. Prior to the participation of 1SOPS, the Research, Development, Test, and Evaluation Support Center at Kirtland Air Force Base in Albuquerque, New Mexico, handled the AFSCN responsibilities.

Figure 13 illustrates the operational timeline over which this interaction occurs. With the current structure of the Space-Surveillance Network there is no full-time real-time access to the SBV sensor. This limits its response to tasking requests to a twenty-four-hour

RADIATION IN SPACE

AT AN ALTITUDE of nine hundred kilometers, the Midcourse Space Experiment (MSX) satellite is continuously exposed to radiation, predominantly in the form of high-energy particles. Since these particles are routinely detected by the Space-Based Visible (SBV) sensor's charge-coupled device (CCD) focal-plane array, much can be learned by investigating the rates and characteristics of these detections. While space science can be studied with these data, this exposure to radiation also leads to both short-term and long-term performance issues for the SBV sensor.

Over time, the accumulation of these radiation events can cause permanent damage to individual detectors or the electronics. The long-term effect can be determined by monitoring three quantities: increases in the dark current level of the SBV sensor, changes in the direct current bias imposed by the instrument's electronics, and reductions in the charge-transfer efficiency of the CCDs. To date, a measurable but small amount of long-term damage to the focal planes has been observed.

In the short term, radiation effects occur on a frame-by-frame basis. High-energy particles strike the SBV focal planes, causing an instantaneous increase in the signal within a pixel. Because these particles, typically protons, travel very quickly, their signals persist for only a single frame. However, since the particles strike the focal plane over a myriad of angles, and since the deposited energy usually bleeds out of the central pixel, the events frequently affect more than one pixel at a time. For this reason, events sometimes appear as short streaklets on the focal plane in a single frame. The primary effect of these events is to increase the apparent temporal noise of the system, but they also affect the ability of the SBV signal processor to distinguish them from a resident space object.

With some exceptions, however, the effect of a radiation event can be removed by deleting the maximum and minimum signal from a set of frames prior to temporal processing. The left image in Figure A shows a typical cover-closed SBV image collected on orbit. Here we see routine radiation events in which one or two pixels are involved, as well as short streaklets. The image is the max-value frame of a sixteen-frame frameset gathered at 1 Hz. The max-value frame displays the maximum signal in the pixel over the entire frameset.

While detections from high-energy protons exist in all SBV framesets, the passage of the MSX satellite through the South Atlantic Anomaly (SAA) yields a substantial increase in the frequency of these detections. The SAA is a region of the earth's magnetic field that displays higher than average densities of trapped charged particles such as protons. The right image in Figure A shows the pro-

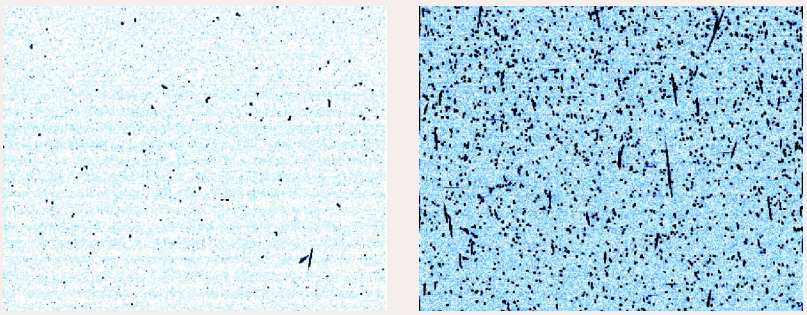

FIGURE A. A cover-closed image from the Space-Based Visible (SBV) sensor (left), and a cover-open image from the sensor when it passes through the South Atlantic Anomaly (SAA) (right). Because of its location near the inner Van Allen radiation belt, the SBV sensor routinely detects protons on its focal-plane array. The SAA, a region of the earth's magnetic field with high levels of trapped particles, inundates the SBV sensor's focal-plane array with proton activity. It is currently not possible to detect and identify RSOs in a reliable manner when the SBV sensor is in such a high-radiation environment.

ton activity during a cover-open pass through the SAA, when the focal-plane array on the SBV sensor is inundated with radiation. It is currently not possible to detect and identify RSOs in a reliable manner in this kind of high-radiation environment.

Figure B shows a time series of the number of radiation events per second on an SBV focal plane, and the average signal strength in digital counts per event. These data were taken as the MSX satellite passed through the SAA. The boundary of the SAA is sharply defined, as indicated by the steep rise in the event rate at 420 seconds into the data collection, and by the rapid decline in the event rate beginning around 1100 seconds. An increase in the average signal strength per event is also evident during this same time. Typically, the event rate rises from an estimated five events per second in regions outside the SAA to a peak greater than a thousand events per second within the SAA. On average, just over four pixels are affected per event. For this pass through the SAA, 28% of the pixels in the focal plane experienced the effects of a single radiation event, while 3% experienced two events [1].

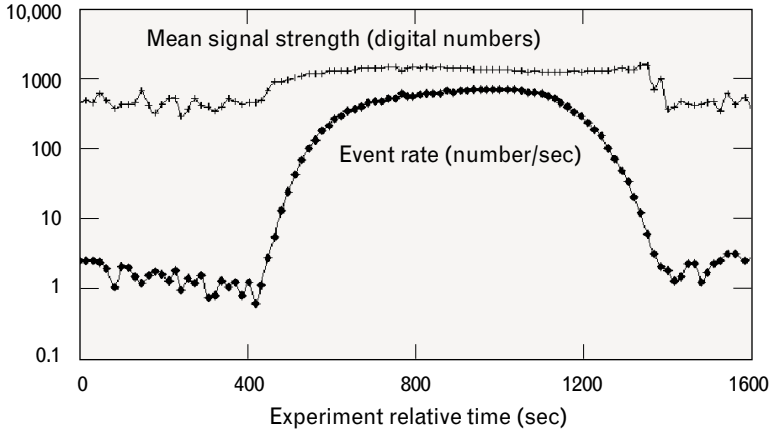

FIGURE B. SBV radiation rates through the SAA. When the SBV sensor is outside the SAA, it detects just a few proton events per second. During a pass of the MSX satellite through the SAA, which occurs during the period from 420 seconds to 1100 seconds, this rate of proton detection exceeds nine hundred events per second, overwhelming the signal processor.

References

1. T.P. Opar, "SBV Data Collections in Support of Space Control," *Proc. 1997 Space Control Conf.* **1**, *Lexington, Mass., 25–27 Mar. 1997,* pp. 11–23 (Lincoln Laboratory Project Report STK-249).

cycle. The timeline is actually comparable to the response time for a GEODSS site, which must wait for nightfall to gather observations [20, 21].

Typically, the tasking list from 1CACS is received in the SPOCC in the early morning, local time. The commands for data collection are then automatically generated for two four-hour events. There are two clusters of contacts with the MSX spacecraft at APL, in the morning (at approximately 8 a.m., local time) and in the afternoon (at approximately 5 p.m., local time). Each cluster consists of either two or three contacts spaced by an orbital period of approximately one hundred minutes. The commands for the first event in the data collection with the SBV sensor are uploaded to the spacecraft during the afternoon cluster of contacts at APL. The data gathered during this event are downloaded during the contact in the morning cluster. The second event starts after the last contact in the morning cluster, during which the data are downloaded during the afternoon cluster at APL or through one of the Space Ground Link System stations at the end of the event.

The length and timing of the data-collection events were chosen for the following three reasons. First, the MSX spacecraft, which was not designed for continuous operation, has successfully demonstrated eight continuous hours of operation. Second, conducting the data-collection events in the afternoon, local time, facilitated the access of the SBV sensor to the region of the geosynchronous belt in the eastern hemisphere (0° to 90° E sub-longitude) where little coverage was provided by the rest of the Space-Surveillance Network. Third, splitting the data collection into two events enabled the tasking commands per

BALLISTIC-MISSILE AND THEATER-MISSILE DATA COLLECTION

THE SBV SENSOR was constructed as a space-based space surveillance sensor on the Midcourse Space Experiment (MSX) satellite, and as such had a number of design elements specific to the mission. The SBV sensor also collected a large amount of data on ballistic-missile launches. The launch data were acquired as full SBV frames recorded on the MSX and downloaded later to ground controllers. The SBV signal processor, tuned for satellite targets, was not used for collecting data on missile targets. The SBV sensor was constructed to provide detection and metric measurements on faint targets. To achieve the best performance for these tasks, the SBV sensor was designed as a broadband sensor and has no spectral capability. It is simply an accurate light bucket that detects as many photons as possible to achieve good SNR on the targets. Given these constraints, the SBV sensor still collected interesting missile launch data that provide insight into the value of using broadband visible focal-plane arrays (FPA) for ballistic-missile defense applications—either jointly with infrared instruments or alone.

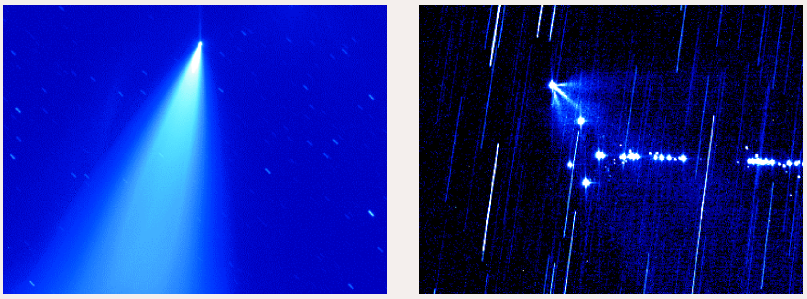

FIGURE A. Raw data taken by the SBV sensor during the boost phase of the MDT II missile launch (left) and later during the deployment phase of the trajectory (right). During the first ten months after the launch of the MSX satellite, the SBV sensor was used to gather metric and photometric data on both ballistic-missile and theater-missile deployments, as well as on RSOs for space surveillance. The MDT II mission was the premier test of ballistic-missile detection for the MSX spacecraft and its sensors.

Compared to existing infrared sensors, the SBV sensor provides two main areas of improved performance. First, at any given level of technology development, visible FPAs may be constructed with more pixels and may be constructed in two-dimensional arrays rather than the linear arrays used in most infrared instruments. Second, the visible FPAs are more sensitive than comparable infrared focal planes. Of course, visible FPAs are unable to detect self-emission from cool targets, and thus are limited to situations when the target is illuminated by the sun. This constraint on visible sensors has generally discouraged their use for ballistic-missile defense applications.

If we are willing to set aside the question of detection of objects in the dark, probably by coupling the visible sensor with an infrared counterpart, the visible sensor can provide useful information for ballistic-missile defense applications. The visible FPAs can provide early detection of objects and ultimate detection of smaller objects, compared to infrared systems of similar aperture size. In addition, the increased resolution and field of view provided by the large number of pixels available in modern visible FPAs allows earlier separation of closely spaced objects across larger complexes.

The MSX Dedicated Target Mission (MDT II) was the premier target mission for the MSX program. The principal objective of this mission was to gather on-orbit infrared, ultraviolet, and visible-band data during the deployment of various reentry-vehicle decoys, balloons, and replicas for studies in discrimination. As part of this mission an intercontinental ballistic missile was launched out of Kauai, Hawaii, into the Kwajalein atoll. The suite of sen-

sors on board the MSX and a host of ground-based sensors tracked the missile and its deployment hardware during the trajectory.

Figure A shows the missile during its early boost phase (left) and during deployment (right). Several detections are present in the deployment image. The streaks interspersed throughout the field are stars passing through the field of view of the SBV sensor. The object in the upper left portion of the complex is the post-boost vehicle (PBV) during a maneuver. This maneuver is evident from the thrust-cone formations of hot hydrazine gas. The PBV has just completed deployment of the collection of objects seen on the right. The balloons are the bright objects to the lower right of the PBV, with the remaining deployed hardware consisting of light reentry-vehicle replicas and a 20-cm black reference sphere (which is located to the left of the center of the large gap in the hardware formation and is fairly faint).

When these images were taken, the range to the complex was approximately a thousand kilometers. Detection of a 20-cm sphere with a reflectivity of 3% at this range clearly demonstrates the sensitivity of the SBV sensor. Careful analysis of the signature data gathered by the SBV sensor on each of these objects yielded compelling evidence that visible-band data can be extremely useful in support of ballistic-missile defense activities.

Two missions similar to the MDT II mission were those associated with the Theater Countermeasures Mitigation Program, or TCMP. While these cooperative missions were not dedicated to MSX data collection, they were executed in coordination with the MSX satellite and other ground-based sensors. Both TCMP I and TCMP II were designed to study discrimination during deployment from tactical theater missiles, much in the same way MDT II did for a strategic missile. Trajectories of both missions went from Wake Island into Kwajalein, and were observed by the SBV sensor during the deployment phase. The range of TCMP IIB was about 3000 km, which is considerably farther than the range of MDT II. As a consequence, details of the deployment are not resolvable by the SBV sensor.

Figure B shows the TCMP IIB complex during the deployment phase. The detection of cold nitrogen gas plumes is evident at this range, even though details of the deployment are not clear. The SBV sensor is actually detecting sunlight reflecting from droplets of liquid nitrogen shortly after the maneuver to deploy the reentry vehicle. This process is revealed by the symmetric ring formation of the gas, which does not form such a pattern during attitude maneuvers. Similar situations were observed in TCMP I and in other cooperative missions as well.

Evidence from these data, as well as data gathered for MDT II and other missions, shows that a wide field-of-view visible-band sensor with high sensitivity can be of great assistance in support of both strategic and theater-missile deployment discrimination.

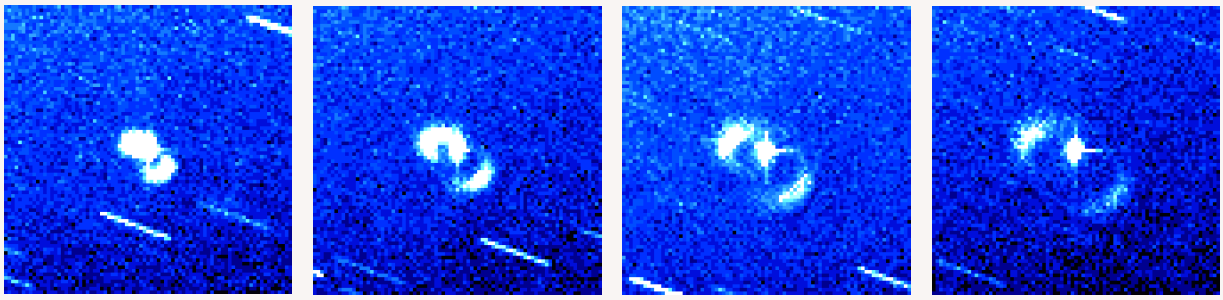

FIGURE B. The TCMP-IIB complex as seen by the SBV sensor. Visible in these images is crystallized nitrogen gas released during the deployment phase of the mission. Because of the large range of the TCMP-IIB complex, the SBV sensor was unable to isolate deployment hardware. By careful analysis of the plume data, however, it was possible to infer the types of maneuvers that occurred, and thus determine information about when hardware was being deployed.

event to be kept within the uplink limits of the spacecraft. Also, at least some RSO observations collected in response to the tasking commands could be sent in a timely fashion to 1CACS by downloading and processing the first-event data.

Typically, each of the data-collection events consists of two parts: geosynchronous search and scheduled response to tasking. Approximately two hours are devoted to search and the remaining six hours are devoted to tasking response. As previously discussed, a significant strength of the SBV sensor is its wide field of view. The geosynchronous belt can be searched at a rate of approximately 50° of longitude per hour by appropriately orienting this field of view. The region searched can also be varied on a daily basis as needed.

Unlike with ground-based sensors, however, there is no real-time access to the SBV sensor. The data-collection events must be planned ahead of time and sent to the operations planning team at APL. The commands are checked for sensor and spacecraft safety before being uploaded to the spacecraft. The planning for a day's event actually starts six to eight weeks earlier, with a process known as monthly planning. The planning is then refined at the weekly level, and the actual set of commands are created at the daily level, in response to that day's tasking list. This cumbersome process is an artifact of the early phase of the mission, when the MSX spacecraft was shared among eight principal investigators. Lack of real-time access limits tasking of the SBV sensor for tactical response. For example, if a new launch occurs, the SBV sensor cannot be tasked for collecting observations on the target until the next day. This lack of real-time access is in contrast to a ground-based sensor, which can respond immediately if the object is above the horizon. Only with fortuitous timing could the SBV sensor respond within several hours.

Because the SBV sensor resides on a six-thousand-pound satellite, repositioning the platform from one attitude to another is a slow process. This fact is illustrated by the following timeline for a single frameset of data collection: (1) reorienting the satellite to the desired attitude (three to five minutes), (2) collecting the data (twelve to twenty-five seconds), (3) signal-processing the data (thirty-five seconds), and (4) orienting the satellite to the next desired attitude (three to five minutes).

Clearly, operating in this mode is quite inefficient. As a consequence, two techniques were developed to help mitigate this problem. First, during geosynchronous search, data are collected and processed from all four of the CCDs, in sequence, before the satellite is reoriented. Second, and more significant, an impor-

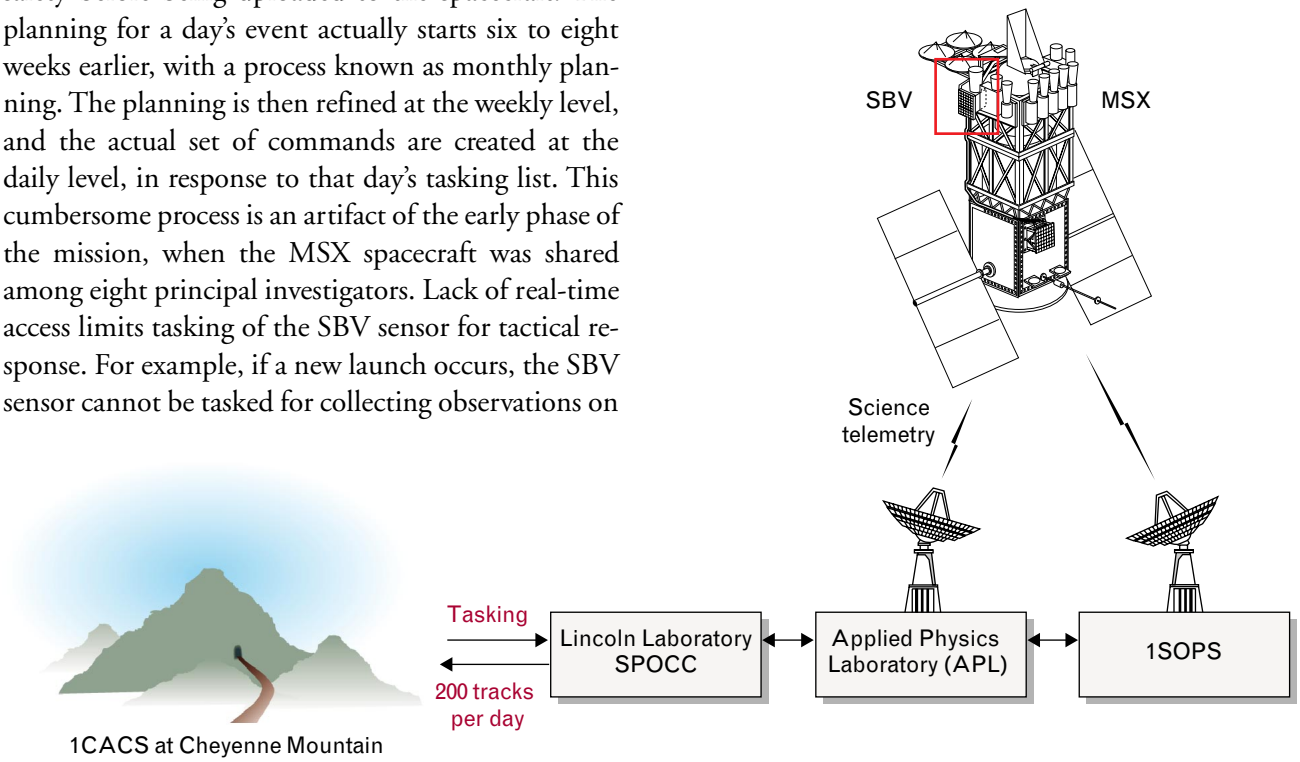

FIGURE 12. The MSX/SBV ground network. The 1st Command and Control Squadron (1CACS) in Cheyenne Mountain, Colorado, the Applied Physics Laboratory (APL) at Johns Hopkins University, the 1st Space Operations Squadron (1SOPS) at Schriever Air Force Base in Colorado Springs, Colorado, and the SBV Processing and Operations Control Center (SPOCC) at Lincoln Laboratory make up the ground-based operations of the MSX satellite and the SBV sensor.

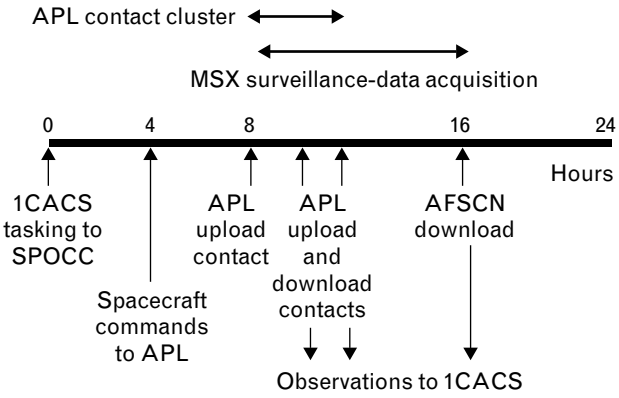

FIGURE 13. Operational timeline for the SBV sensor as a Contributing Sensor. One of the goals of the Advanced Concept Technology Demonstration (ACTD) is to provide timely response of the SBV sensor to daily tasking requests from 1CACS in Cheyenne Mountain. The timeline shows the breakdown of activities from the receipt of tasking requests in the SPOCC, to the downlinks through the Air Force Satellite Control Network (AFSCN), and finally to the transmission of observations from the SPOCC to 1CACS.

tant piece of software for choosing some optimal scheduling of objects was redesigned with the strengths of the SBV sensor in mind. The conjunction-optimized look-ahead (COLA) scheduler takes the submitted tasking list of objects to view on any given day and seeks out regions of space in which RSOs are in apparent conjunction with any two of the four CCDs. With this design, the SBV sensor typically sees at least two objects per CCD, and enables sequential operations similar to that of geosynchronous search.

The COLA Scheduler

The SBV sensor is an inherently wide field-of-view instrument, as described earlier. Each CCD covers approximately $1.4° \times 1.4°$, and all four CCDs together cover a total field of regard of $6.6° \times 1.4°$. It is immediately evident that the SBV sensor can use this wide coverage to increase productivity when tracking the previously mentioned geosynchronous clusters. However, a small study indicated that the SBV sensor was capable of detecting spatially clustered nongeosynchronous deep-space RSOs as well. Figure 8 illustrates an example of this effect, in which the SBV sensor detected a low-earth-orbit satellite, a high-earth-orbit satellite, and three geosynchronous-orbit satellites within the same field of view—all in an apparent conjunction. The COLA scheduler was written to take advantage of such conjunctions in scheduling so as to maximize the productivity of the SBV sensor and enhance its utility to Space Command [22, 23].

Space-surveillance operations depend on timely and reliable data flow on observations of RSOs. Hence it is vital to have sensors available seven days per week. The SBV sensor, under its previous paradigm as an experimental sensor, was operated five days per week and only for short periods, typically twenty minutes in duration. As a Contributing Sensor to the Space-Surveillance Network, however, the SBV sensor is operated seven days per week, with one of those days reserved for maintenance and developmental activities.

The time series shown in Figure 14 gives the history of the productivity of the SBV sensor during the early transition experiments. The space-surveillance interface processor, or SSIP, was the standard scheduler in the early days, with no optimization for conjunctions. The distinct improvement in productivity with the COLA scheduler is evident in Figure 14 beginning in April 1998. Clearly, the use of temporal, spatially apparent conjunctions of satellites in a wide field of view is an effective technique for enhancing the productivity of the SBV sensor, and by extension any wide field-of-view sensor [22].

The impact of the COLA scheduler on overall productivity has been substantial, as shown in Figure 14. This impact is even more striking when viewed in terms of the SBV sensor's overall contribution to the Space-Surveillance Network. A principal question of interest with regard to any new sensor is how the new sensor will perform relative to other sensors within the network. This question is addressed in Figure 15, in which overall productivity in terms of total observations is shown for the SBV sensor; the three ground-based GEODSS sites at Socorro, Diego Garcia, and Maui; the Lincoln Laboratory–developed Transportable Optical System (TOS) ground sensor; and the Maui Space-Surveillance System (MSSS). The figure clearly indicates that the SBV sensor is competitive with all three ground-based GEODSS sites. It should also be noted that the SBV sensor is a single telescope with a fifteen-centimeter aperture,

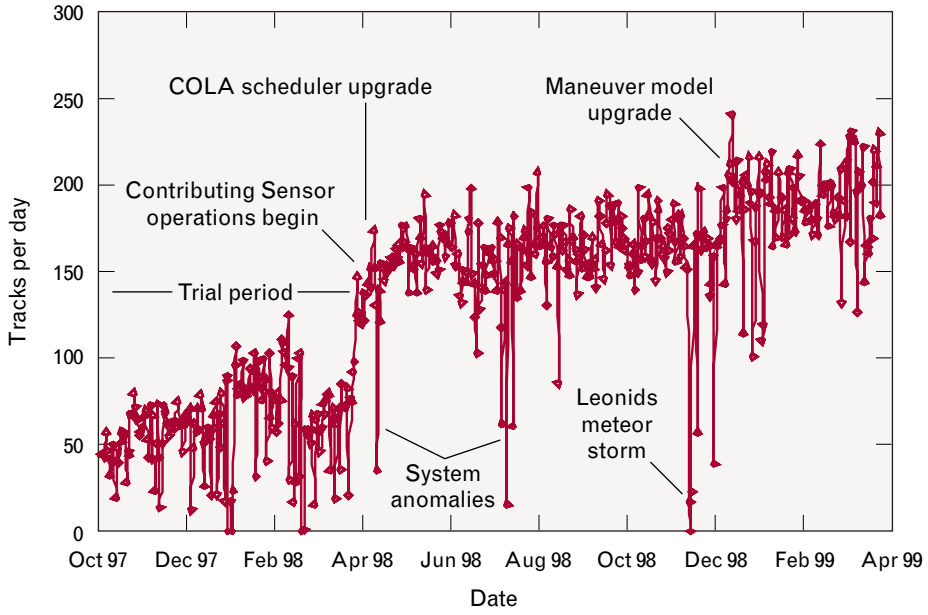

FIGURE 14. Effects of productivity-enhancement techniques on satellite tracking. The SBV ground-processing system in the SPOCC went through several upgrades in preparation for the commencement of Contributing Sensor operations in April 1998. An earlier space-surveillance processor had no optimization for conjunctions. The conjunction-optimized look-ahead (COLA) scheduler, which is used today, optimizes the submitted list of tasking commands and seeks out regions of space in which RSOs are in apparent conjunction with any two of the four CCDs in the SBV sensor. Currently, as a result of these enhancements, the SBV sensor is producing over two hundred tracks per day on deep-space satellites, which is twice the original goal of the ACTD.

while the GEODSS telescopes have one-meter apertures and multiple telescopes per site [20].

RSO Catalog Maintenance

Finally, one of the most significant contributions that the SBV sensor has made to Space Command and the maintenance of the RSO catalog is the reduction of the average age of an element set within the catalog. The element set associated with any object in the catalog is used to point sensors within the Space-Surveillance Network to gather more tracking data on that object. The tracking data from all the sites are then merged, and after the orbit-determination process is completed, the element set is updated. If the element set is not updated in a timely manner, there is a risk that the pointing information sent to the sensors will not be sufficiently accurate to place the object within the field of view, or beamwidth, of the instrument. If no sensor can find the object, its element set will continue to degrade and the object will be effectively lost from the RSO catalog.

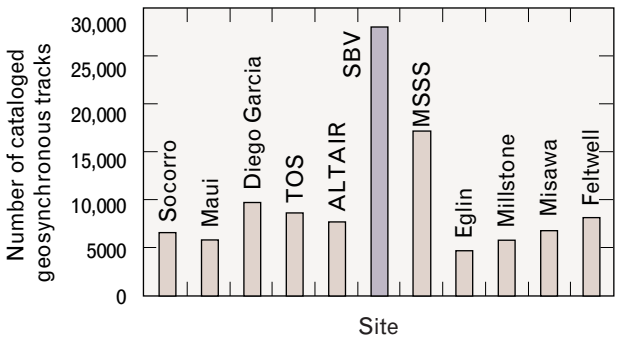

FIGURE 15. Number of tracks on cataloged geosynchronous satellites for the SBV sensor; the three GEODSS optical sites at Socorro, Maui, and Diego Garcia; the Lincoln Laboratory–developed Transportable Optical System (TOS) ground sensor; and six additional ground-based radar sites from April to December 1998. Principally because of its position on orbit, its wide field of view, and the design of the COLA scheduler, the SBV sensor is the most productive deep-space optical sensor in the Space-Surveillance Network for tracking geosynchronous satellites. The GEODSS sites share their time between near-earth and deep-space tracking of RSOs, however, while the SBV sensor is primarily dedicated to tracking RSOs in the geosynchronous belt.

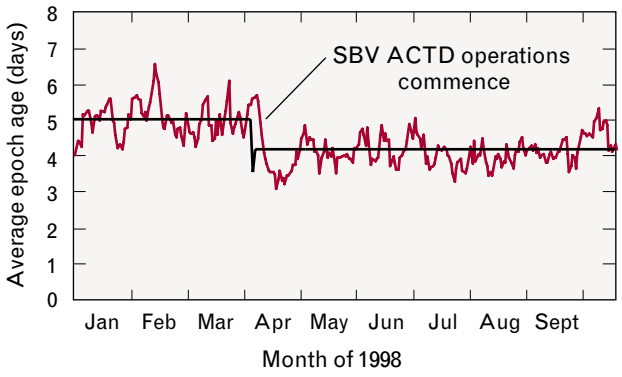

FIGURE 16. The contribution of the SBV sensor to the average age of an element set within the RSO catalog. When the SBV sensor commenced operations in April 1998, a clear and significant decrease occurred in the average age of an element set in the catalog. The decline resulted from the addition of the SBV sensor to the Space-Surveillance Network and from the tracking of older satellites by the SBV.

This problem can also occur if the object performs a significant maneuver and the sensors do not gather tracking data on it in a timely manner. As a consequence, element sets should be updated frequently. This updating could be accomplished through more efficient use of existing resources in the Space-Surveillance Network, or by adding a sensor to the network (which was the case with the SBV sensor). Figure 16 shows the impact on the average age of an element set when the SBV sensor became operational in April 1998. The introduction of a single space-based sensor reduced the average age of an element set in the RSO catalog by 20% [20].

Signal Processor Software Enhancements

The SBV sensor has an onboard signal processor that distills several frames of full-bandwidth CCD data into a few stars and a few satellite streaks, as illustrated earlier in Figure 4. The CCD camera collects a series of raw frames, or exposures, and transmits them to the signal processor. The signal processor then extracts a set of stars and the streak end points from the camera data, and those extracted data are downloaded to the SPOCC. In general this process has worked well, although some difficulties have occurred. Since the MSX satellite is situated near the inner Van Allen radiation belt, protons emanating from the sun are often detected by the CCDs on the SBV sensor, as described in the sidebar entitled "Radiation in Space." These proton events are manifested as short, bright detections that under certain conditions can either corrupt the formation of an RSO streak or, in some cases, appear to the signal processor like a valid streak.

Figure 17 shows an example of two such proton detections. The frameset in the figure was taken with the cover of the SBV telescope closed. Thus all star-like and streak-like apparitions in the frameset are caused by proton events on the focal plane. The number of such events varies from as few as four events per frame in benign regions of the orbit to as many as nine hundred events per frame in the South Atlantic Anomaly. Approximately 32% of the framesets collected by the SBV sensor show false streaks due to such proton events.

Filtering out false streaks due to proton events is currently done by processing software on the ground. Figure 18 compares the characteristic signatures of a false streak caused by a proton event and a valid streak caused by an RSO. The proton event is a temporally short bright event, clearly unlike the signature left by a typical RSO. Software has been added to the ground-based data-reduction process to detect and

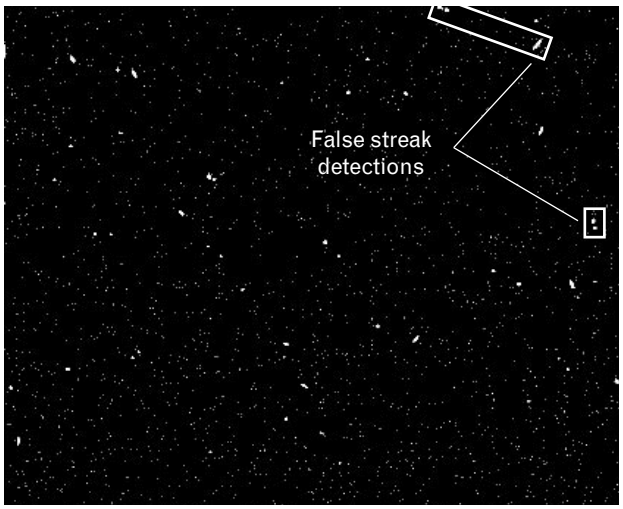

FIGURE 17. A frameset with the cover of the SBV sensor closed, showing false streak detections caused by proton events. Protons, which are always present in SBV framesets, usually have event signatures that are significantly different from those of RSOs. Under certain conditions, these proton detections are registered as valid streaks by the signal processor, and they must be filtered by both on-orbit and ground-based software prior to the data-reduction process.

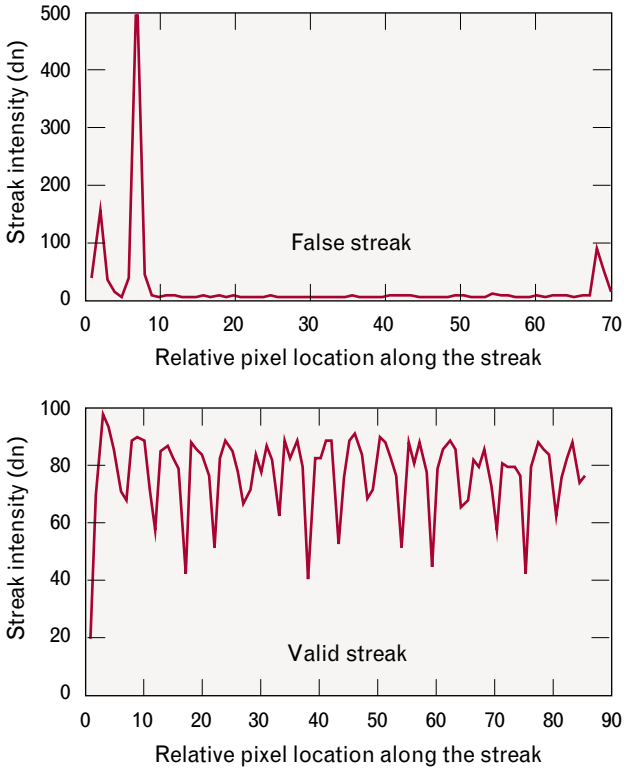

FIGURE 18. Characteristic intensity signatures, given in digital numbers (dn), of a false streak caused by a proton event (top) and a valid streak caused by an RSO (bottom). By analyzing variations in pixel intensities across the entire streak, ground-based processing software can distinguish false streaks from valid streaks.

remove false streaks on the basis of these differences in characteristic signatures [16, 22].

Tests on the ground have shown that two additional problems occur because of the proton events. Proton events can overlie valid streaks, in which case the detected streak can be corrupted and the suppression algorithm described above fails. In addition, data collection in a region of intense proton events can overwhelm the signal processor, rendering it unable to detect any streaks. These problems can be corrected only by modifications to the onboard processing software in the signal processor. This modified software was developed and tested on the ground, and Table 1 shows the results of this testing.

We examined 195 framesets, or looks, and we processed streaks through both the old signal processing software and the revised signal processing software. As the table shows, the number of detected streaks actually decreased with the implementation of the revised signal processor code, a result that occurred entirely because of the substantial reduction in the percentage of false streaks detected. It is also evident from the table that the actual number of valid streaks increased with the revised software. Both of these results achieve the desire outcome—a higher percentage of object detections. Because of the positive results of ground-based testing, we uploaded the revised signal processing software to the MSX spacecraft and significantly improved the performance characteristics of the SBV sensor [22].

Software System and Automation

The SBV Processing Operations and Control Center (SPOCC) utilizes an intricate, highly complicated software system for processing sensor data. Figure 19 illustrates the architecture of the system. Since the SPOCC operates seven days a week, eight hours a day, the system must be highly automated to mini-

Table 1. Differences in Streak Processing for Old and New Signal Processing Software*

	Number of Looks	*Number of Streaks*	*False Streaks*	*Number of Valid Streaks*
Old signal processing software	195	298	41%	177
New signal processing software	195	241	15%	204

* Following launch and an initial analysis of the streak data, we determined that false streaks could be reduced on board, prior to downloading, if the signal processor was reprogrammed. New signal processing software was developed and uploaded to the MSX spacecraft, resulting in a reduction in the number of false streaks and an increase in the number of valid streaks.

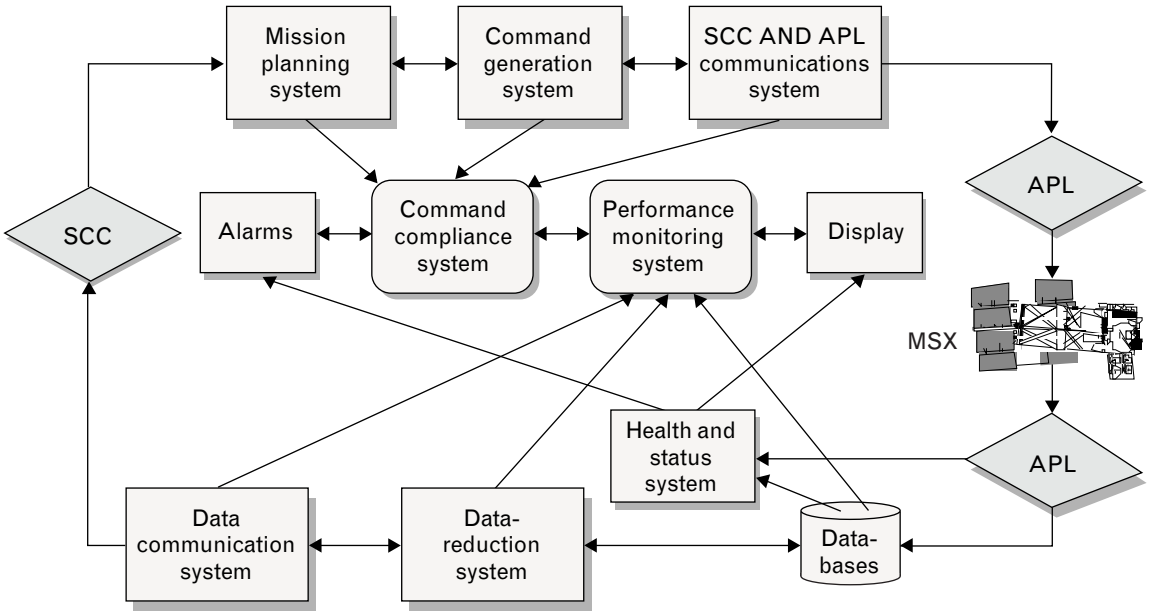

FIGURE 19. SPOCC software architecture. The end-to-end processing of SBV data begins with the Space Control Center (SCC) tasking requests (far left) and progresses through mission planning, command generation, upload to the MSX satellite, data collection, telemetry download, data reduction, and sensor and network monitoring. The system is highly automated to reduce costs.

mize costs and ensure reliable and repeatable performance of the SBV sensor. As a result, from the first steps in mission planning to the final transmission of observations to Space Command, human intervention is rarely required. A substantial number of system performance points are monitored for errors, and a robust paging system has been established to bring serious problems to the attention of operators in a timely manner. The paging system, in addition to a health and status information system monitoring the performance of the SBV sensor, gives operators keen insight into the location of a problem, thus allowing for rapid diagnosis and correction. A complement of visual displays and checkpoints allow efficient access to this information [19].

Data Reduction

Twice every day, the signal-processed data are downloaded from the MSX spacecraft and delivered to the SPOCC at Lincoln Laboratory. The first step in the processing of the data is referred to as decommutation, in which relevant information from the telemetry data stream is extracted and archived in a database. The data-reduction process is responsible for determining the boresight pointing for the sensor, establishing the streak end point locations of the detected RSOs in terms of absolute angles on the sky (right ascension and declination), and correlating the streaks to the catalog of known objects. This process was discussed in detail earlier in this article. As with the entire SPOCC software system, the data-reduction process is automated and is triggered when the decommutation of the telemetry data is complete.

Health and Status

Telemetry data for monitoring the health and status of the SBV sensor are downloaded ten to fifteen times per day, through both the APL and Space Ground Link System stations. The data are automatically processed, archived, and limit checked. The health and status data from every contact are also automatically displayed with appropriate colors to indicate status of any particular subsystem on the instrument. The operator's display uses a standard green-yellow-red monitoring system; the color gray indicates when redundant components are unpowered. The archived data are later processed with trending software to assess long-term behavior [19].

Daily SPOCC Operations

The operation of the MSX satellite and the SBV sensor, shown earlier in Figure 12, is as follows. The 1st Command and Control Squadron (1CACS) of Space Command generates the tasking at the Space Control Center in Cheyenne Mountain and forwards it to the SPOCC at Lincoln Laboratory via the communications node at the Millstone Hill radar. The SPOCC schedules operations in response to the 1CACS tasking list and generates commands that will implement SBV operations on the MSX satellite. The SPOCC mission-planning process is highly automated and is operated by a minimal staff. The automated process takes into account all of the constraints, capabilities, and issues related to resources on board the MSX spacecraft. The commands are sent via electronic link to APL for inclusion in the MSX upload, and are uplinked by APL to the MSX spacecraft. The data on targets are then acquired by the SBV sensor and the results are stored in a RAM buffer on board the SBV until a 1-Mbit/sec downlink is available. Downlinks can be accomplished via the APL dedicated station or the Space Ground Link System network.

Data are returned to the SPOCC at Lincoln Laboratory for processing into observations in the standard Space Command format. The observations are delivered to 1CACS in Cheyenne Mountain via the existing link connecting Millstone Hill to the Space Control Center. The SPOCC is also responsible for the generation of the MSX ephemeris and SBV sensor health and status monitoring. The SBV sensor is now operated seven days per week, with one day per week allowed for routine maintenance and development. During the technology demonstration phase, the operations of the SBV sensor and the SPOCC were quite similar except that the tasking list came from the Surveillance Principal Investigator team.

The goal of producing one hundred tracks per eight-hour day during full operations was set for the SBV sensor in the ACTD proposal process. As of this writing, the SBV sensor is supplying more than two hundred tracks per eight-hour day; this higher number of tracks is the result of a number of previously discussed improvements undertaken to increase the productivity of the sensor [19, 24, 25].

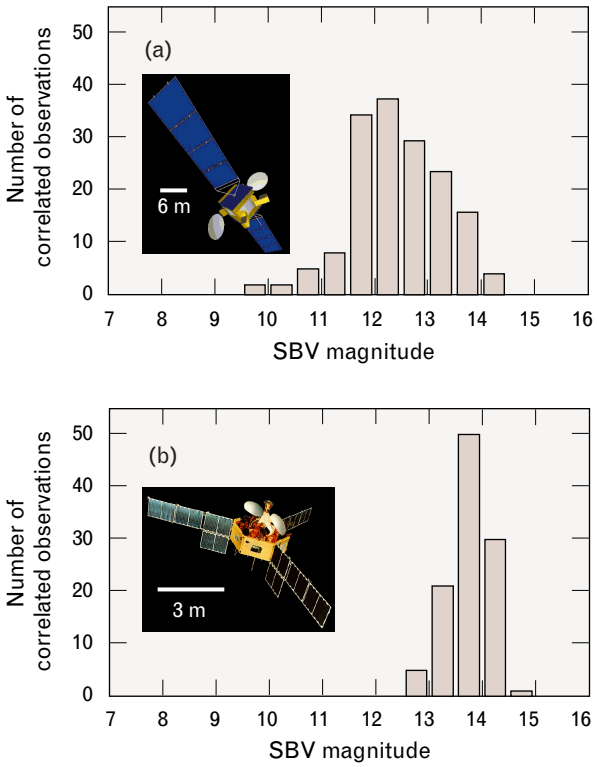

FIGURE 20. (a) Observed magnitude of Telstar 401 satellite (22977); (b) observed magnitude of relatively smaller Symphonie A and B satellites (7578 and 8132). The magnitude or brightness of a satellite depends on a variety of parameters, including its size and composition, the relative geometry with the sun, and the satellite's orientation. As a consequence, the monitoring of a satellite's brightness can reveal information about whether it is stable or tumbling. The SBV sensor is able to track satellites as faint as 15th magnitude, or the equivalent of about 0.5 m^2 in effective cross section (reflectivity multiplied by actual cross-section area) at geosynchronous altitude.

SBV Photometry

As discussed earlier, the SBV sensor produces information on the brightness of an object, and at the same time the sensor establishes an object's metric position. Figure 7 shows that the brightness is determined from the pixel intensities detected by the CCD focal-plane array and quantified in terms of a visual magnitude called the SBV magnitude. The SBV sensor was originally designed to achieve a photometric sensitivity of 14.5, in terms of SBV magnitude. The actual demonstrated capability on orbit, however, was shown to exceed 15th magnitude. The detections included in Figure 7 are only those made by the SBV

which were successfully correlated to known objects in the RSO catalog.

While the principal contributing aspect of any sensor within the Space-Surveillance Network is metric information, a great deal of additional information can be gleaned from the photometric signature of an RSO as well. The photometric signature is instrumental to the ground processing of the SBV data to achieve high metric accuracy, but the brightness of an object can also be used to discriminate objects on the basis of size, configuration, reflectivity characteristics, and status. Figure 20 contains pictorial representations of two satellites—one significantly larger than the other—and a histogram of SBV photometric observations on each. As expected, these two diagrams show that, when normalized by range, smaller objects appear less bright than larger objects.

A common measure describing the relative geometry between a target satellite, the observing sensor, and the sun is referred to as the phase angle. Figure 21 illustrates the geometry of the phase angle. By repeatedly observing a given satellite over a range of phase angles, we can determine a characteristic phase curve. The phase curve of an object displays characteristic features that can be used photometrically to indicate classes of satellites or to discriminate within classes. For example, the stability of a three-axis stabilized spacecraft can be determined by using this technique.

Figure 22 shows such an example, in which photometric data on both a stable and an unstable Hughes HS-601 class satellite is given as a function of phase angle. Active three-axis stabilized satellites typically have large solar panels that track the sun. When photometric observations are made of these satellites at small phase angles, the solar panels of stable satellites provide a bright reflection, as can be seen by the decreasing magnitude (i.e., brighter) signature as phase angle decreases in Figure 22(b). The solar panels of unstable satellites, however, no longer track the sun and thus show no such trend in magnitude as phase

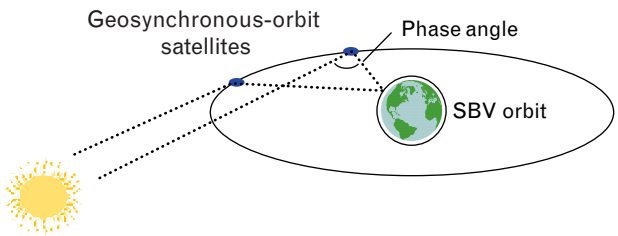

FIGURE 21. Geometry of space-based photometric observations. The phase angle, which is determined by the relative orientation of the sun, the SBV sensor, and the target, plays a vital role in our ability to detect satellites on orbit. The SBV sensor is able to track geosynchronous-orbit satellites with phase angles as high as 100°.

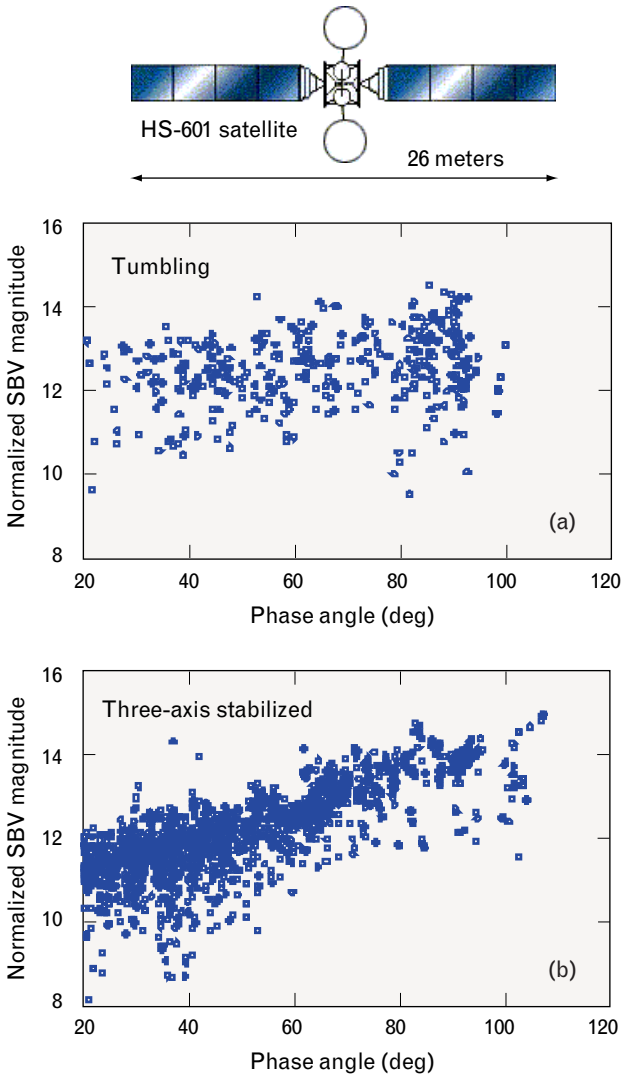

FIGURE 22. Photometric data as a function of phase angle for (a) an unstabilized Hughes HS-601 satellite and (b) a three-axis stabilized HS-601 satellite showing detectable difference. Geosynchronous satellites are typically stabilized in a nadir-pointing orientation. As a consequence, their phase curves display highly linear behavior, as shown in part *b*. If the satellite is tumbling, however, all sides of the spacecraft return reflected sunlight, and the brightness of the satellite tends to appear constant as a function of phase angle, as shown in part *a*.

angle varies, as shown by the relatively constant magnitude signature in Figure 22(a). An example such as this demonstrates how photometric measurements over a range of phase angles can be used to determine the status of satellites [26].

As these results indicate, data from the SBV sensor can be used to obtain information on the operational state of satellites and can aid in their identification. Both of these capabilities—operational status and object identification—are useful to Space Command in conducting space-surveillance operations.

Summary

The SBV sensor has achieved its primary objective of demonstrating space-based space-surveillance operations. The success of the SBV sensor in the technology-demonstration phase has resulted in the incorporation of the sensor into the operational Space-Surveillance Network as a Contributing Sensor. When operating as a Contributing Sensor eight hours per day, the SBV sensor has proven to be as productive as a GEODSS ground-based site with respect to the number of observations gathered. The SBV sensor also produces considerably more accurate observations than those produced by a GEODSS sensor. In addition, the SBV sensor has had a quantifiable impact on the maintenance of the RSO catalog with regard to overall productivity and the average age of an element set. Furthermore, the SBV program has demonstrated the successful operation of a wide range of technologies, including staring focal planes, high off-axis rejection optics, and on-orbit signal processing. An effective concept of operations has been developed for space-based space surveillance, implemented in a highly automated way in the SPOCC, and validated under the current space-based space-surveillance operations ACTD program.

The success of the SBV program has been achieved by understanding the needs of the operational elements of Space Command, and taking a systems approach to developing an effective solution to the requirements of Space Command operators.

Acknowledgments

The construction and initial operation of the SBV sensor were sponsored by the Air Force Space and Missile Systems Center, in the Space-Based Infrared Systems Program Office. Operations of the SBV sensor as a Contributing Sensor under the Space-Based Space-Surveillance Operations ACTD are sponsored by the Ballistic Missile Defense Organization, Air Force Space Command, and the Office of the Secretary of Defense for Advanced Technology.

REFERENCES

1. E.M. Gaposchkin, C. von Braun, and J. Sharma, "Space Based Space Surveillance with SBV," *Proc. 1997 Space Control Conf.* **2,** *Lexington, Mass., 25–27 Mar. 1997,* pp. 73–85 (Lincoln Laboratory Project Report STK-249).
2. E.M. Gaposchkin, "Space-Based Space Surveillance with MSX," *Spaceflight Mechanics 1995: Proc. AAS/AIAA Spaceflight Mechanics, Albuquerque, N.Mex., 13–16 Feb. 1995,* pp. 1681–1690.
3. J.D. Mill, R.R. O'Neill, S. Price, G.J. Romick, O.M. Uy, E.M. Gaposchkin, G.C. Light, W.W. Moore, Jr., T.L. Murdock, and A.T. Stair, Jr., "Midcourse Space Experiment: Introduction to the Spacecraft, Instruments and Scientific Objectives," *J. Spacecr. Rockets* **31** (5), 1994, pp. 900–907.
4. T.P. Opar, "SBV Data Collections in Support of Space Control," *Proc. 1997 Space Control Conf.* **1,** *Lexington, Mass., 25–27 Mar. 1997,* pp. 11–23 (Lincoln Laboratory Project Report STK-249).
5. T.P. Opar, "Calibration and Characterization of the SBV Sensor," *Proc. 1993 Space Surveillance Workshop* **2,** *Lexington, Mass., 30 Mar.–1. Apr. 1993,* pp. 1–7 (Lincoln Laboratory Project Report STK-206).
6. J.C. Anderson, G.S. Downs, and P.C. Trepagnier, "A Signal Processor for Space-Based Visible Sensing," *SPIE* **1479,** 1991, pp. 78–92.
7. J.C. Anderson, "Cost-Reduction Techniques for Low Earth-Orbit Signal Processors," *Int. Conf. on Signal Processing Applications and Technology* **1,** *Boston, 2–5 Nov. 1992,* pp. 228–234.
8. P.L. Chu, "Efficient Detection of Small Moving Objects," MIT Lincoln Laboratory Technical Report TR-846 (21 July 1989), DTIC #AD-A213314.
9. C. von Braun, J. Sharma, and E.M. Gaposchkin, "SBV Metric Accuracy," *Proc. 1997 Space Control Conf.* **2,** *Lexington, Mass., 25–27 Mar. 1997,* pp. 49–62 (Lincoln Laboratory Project Report STK-249).
10. J. Sharma, C. von Braun, and E.M. Gaposchkin, "SBV Data Reduction," *Proc. 1997 Space Control Conf.* **2,** *Lexington, Mass., 25–27 Mar. 1997,* pp. 37–48 (Lincoln Laboratory Project Report STK-249).
11. E.M. Gaposchkin, M.T. Lane, and R.I. Abbot, "Reduction Procedures for Accurate Analysis of MSX Surveillance Experiment Data," *Flight Mechanics/Estimation Theory Symp., Greenbelt, Md., 17–19 May 1994,* pp. 63–76.
12. R.I. Abbot, E.M. Gaposchkin, and C. von Braun, "MSX Precision Ephemeris," *Proc. 1997 Space Control Conf.* **2,** *Lexington, Mass., 25–27 Mar. 1997,* pp. 63–71 (Lincoln Laboratory Project Report STK-249).
13. R.I. Abbot, C. von Braun, and G.E. Powell, "MSX Precision Ephemeris Generation," *Spaceflight Mechanics 1995: Proc. AAS/AIAA Spaceflight Mechanics Conf., Albuquerque, N.Mex.,*

13–15 Feb. 1995, pp. 1711–1722.

14. C. von Braun, "Cryogen Thrust Modeling for MSX Ephemeris Generation," *Spaceflight Mechanics 1996: Proc. 6th AAS/AIAA Spaceflight Mechanics Conf., Austin, Tex., 12–15 Feb. 1996,* pp. 309–323.
15. C. von Braun and E.M. Gaposchkin, "Improvements to SBV Metric Accuracy Using Spacecraft Drift Corrections," submitted to *AIAA J. Guidance, Control & Dynamics,* 1998.
16. J. Sharma, "SBV Space Surveillance Performance," submitted to the 1998 Space Control Conference, Lincoln Laboratory, Lexington, Mass. 15–17 Apr. 1998 (Lincoln Laboratory Project Report STK-253).
17. G. Stokes, "SBV Program Overview," *Proc. 1997 Space Control Conf.* **2,** *Lexington, Mass., 25–27 Mar. 1997,* pp. 17–23 (Lincoln Laboratory Project Report STK-249).
18. G.R. Zollinger, J. Sharma, and M.J. Lewis, "SBV Uncorrelated Target (UCT) Processing," *Proc. 1999 Space Control Conference, Lexington, Mass., April 13–15*, pp. 175–188 (Lincoln Laboratory Project Report STK-254).
19. H.E.M. Viggh, D.J. Blaufuss, F.E. Morton, Jr., A.J. Wiseman, and R. Sridharan, "SPOCC Mission Planning System Performance," *Proc. 1997 Space Control Conf.* **2,** *Lexington, Mass., 25–27 Mar. 1997,* pp. 25–35 (Lincoln Laboratory Project Report STK-249).
20. C. von Braun, "SBV Metric Accuracy," *Proc. 1999 Space Control Conference, Lexington, Mass., April 13–15*, pp. 147–162 (Lincoln Laboratory Project Report STK-254).
21. G.H. Stokes and A. Good, "Joint Operations Planning for Space Surveillance Missions on the MSX Satellite," *Third Int. Symp. on Space Mission Operations and Ground Data Systems, Pt. 1, Greenbelt, Md., 15–18 Nov. 1994,* pp. 319–326.
22. R. Sridharan, B. Burnham, and A. Wiseman, "Performance Improvements of the SBV," *Proc. 1998 Space Control Conference, Lexington, Mass., April 14–16*, pp. 71–80 (Lincoln Laboratory Project Report STK-253).
23. W.F. Burnham and R. Sridharan, "Geosynchronous Surveillance with a Space-Based Sensor," *Spaceflight Mechanics 1996: Proc. AAS/AIAA Spaceflight Mechanics Conf., Austin, Tex., 12–15 Feb. 1996,* pp. 1693–1695.
24. R. Sridharan, G. Duff, A. Hayes, and A.J. Wiseman, "A Feasibility Analysis System for Surveillance Experiments with MSX," *Proc. 1994 Space Surveillance Workshop* **1,** *Lexington, Mass., 5–7 Apr. 1993,* pp. 35–51 (Lincoln Laboratory Project Report STK-221).
25. R. Sridharan, T. Fishman, E. Robinson, H.E.M. Viggh, and A. Wiseman, "Mission Planning for Space-Based Satellite Surveillance Experiments with the MSX," *Third Int. Symp. on Space Mission Operations and Ground Data Systems, Pt. 1, Greenbelt, Md., 15–18 Nov. 1994,* pp. 295–303.
26. R. Lambour, R. Bergemann, C. von Braun, and E.M. Gaposchkin, "SBV Space Object Photometry: Initial Results," submitted to the 1998 Space Control Conf., Lincoln Laboratory, Lexington, Mass, 15–17 Apr. 1998 (Lincoln Laboratory Project Report STK-253).

APPENDIX 1: SBV HARDWARE

THE SBV SENSOR HARDWARE, shown in Figure 1, was designed and integrated at Lincoln Laboratory, and a number of the components were fabricated at the Laboratory in the late 1980s under stringent cleanliness and functionality requirements. This appendix provides a detailed look at the SBV sensor hardware. A companion appendix on system integration and testing provides details on how the SBV sensor was tested and calibrated to achieve the impressive capability demonstrated on orbit. (Note: these two appendices contain updated versions of material that was originally published in the *Johns Hopkins APL Technical Digest* [1].)

Figure 2 shows a diagram of the components of the SBV sensor [1]. The sensor is located in two zones—the instrument section and the electronics side assembly. The telescope and focal-plane assembly, the telescope aperture cover and controller, and the CCD camera are in the instrument section, which is located on the forward section of the spacecraft. The signal processor, the experiment controller, the power conditioner, and the telemetry interface to the spacecraft are in a single assembly called the electronics side assembly, which is located in the aft section of the spacecraft. Figure 3 illustrates the relative locations of the components of the SBV sensor [1–3].

Telescope

The telescope was developed by SSG, Inc., Waltham, Massachusetts. It employs a three-mirror anastigmat, off-axis reimaging design to maximize stray-light rejection of bright sources such as the sunlit earth, which may be just outside the field of view of the telescope. This design configuration introduces well-defined spatial distortions, which are considered a tradeoff for good focusing characteristics [4].

The total field of view of the telescope, including distortions, is around $1.4° \times 6.6°$ with four CCDs in the focal plane. Each pixel has a near-square field of view of approximately 60 μrad on a side; local distortions vary the size of the pixel field of view from the nominal. An aperture cover, opened and closed on command, is used for contamination control, thus preventing dirt accumulation during launch and on orbit when the SBV sensor is not being used. The cover has a secondary mechanism that can open the cover permanently if the normal mechanism fails.

Focus quality and stability became an issue early in the development and construction of the SBV sensor. Initial results describing problems with the Hubble telescope were published just before the SBV sensor's Critical Design Review. To maintain focus independent of operating temperature, the telescope housing and mirrors were made of the same type of aluminum, resulting in an athermal system. All elements expand or shrink at the same rate, keeping the focal plane in a fixed location. Plate scale and distortion maps are expected to change with temperature, and computer modeling indicated that it was important to keep temperature gradients low, thus making athermal assumptions valid. Thick walls, thick mir-

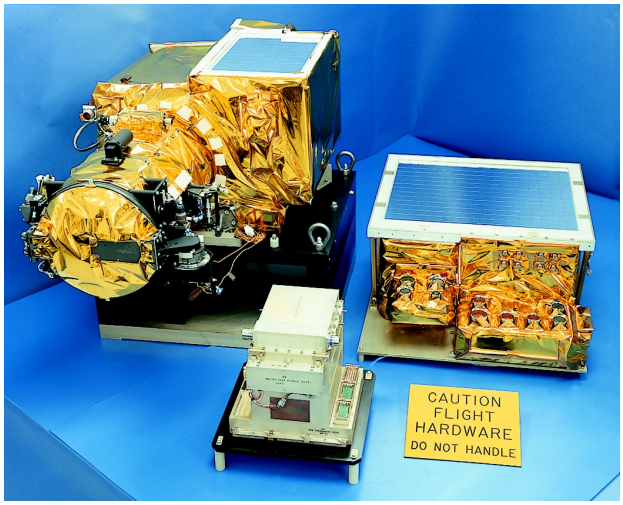

FIGURE 1. SBV sensor hardware. The telescope assembly was built by SSG Inc., Waltham, Massachusetts, and the focal-plane array, the CCD camera, the signal processor, and other components of the SBV sensor were fabricated at Lincoln Laboratory. Integration, testing, and calibration of the SBV sensor were performed in the Engineering division and the Aerospace division at Lincoln Laboratory.

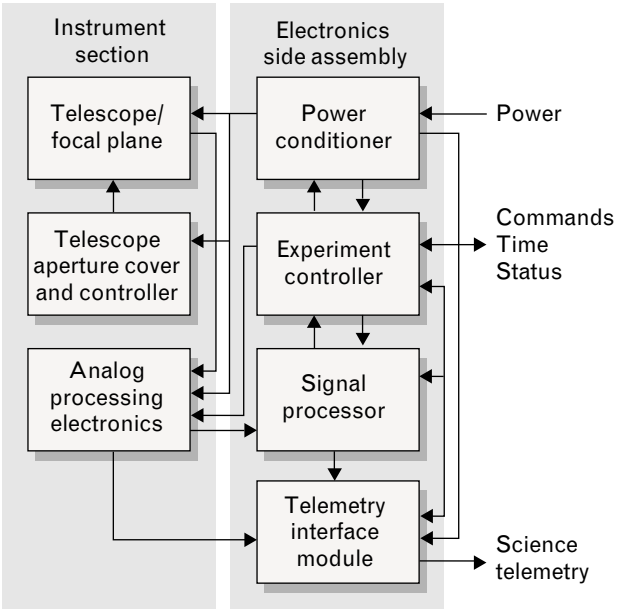

FIGURE 2. Components of the SBV sensor hardware are separated into two zones. The telescope and analog processing electronics are in the instrument section on the top of the MSX satellite, along with the other sensors, while the signal processor, experiment controller, telemetry interface module, and power conditioner are in the electronics side assembly in the rear of the MSX. Reprinted from the *Johns Hopkins APL Technical Digest* by permission [1].

rors, thermal isolation from the spacecraft mounting surface, and a multilayer insulation blanket were incorporated into the design to keep gradients well below the design allowable limits of 3.5°C. Focus is specified as an ensquared energy percentage, which is the percent of total energy in the central pixel after optimum centering. The ensquared energy limit was set to be no less than 50% to maximize detection probability and no more than 80% to allow ground analysis of star centroids for subpixel pointing determination by a slight oversampling of point sources.

A significant challenge for the SBV program is to keep the telescope optics clean up to, during, and after launch. The first two mirrors are superpolished with gold surfaces to maintain low scatter characteristics. Our process to maintain cleanliness covers three areas—design, handling, and operation. The design of the telescope eliminates penetrating holes inside the optical cavity. On the ground, the telescope aperture cover was opened only in a Class-100 clean tent or a vacuum chamber. A continuous dry nitrogen purge was maintained, even during shipping, until just before launch [5].

Focal Plane

The SBV focal plane is comprised of a 1×4 array of Lincoln Laboratory–fabricated frame-transfer visible-light CCD imagers, which were specifically developed for space surveillance. The CCD imagers are mounted on a ceramic substrate for electrical interconnects; the substrate is then bonded to a Kovar tray (Kovar is an iron alloy commonly used in semiconductor packages). A thermoelectric cooler controls the temperature of the focal plane. The focal plane is read out in a sequential mode, one imager at a time, at a pixel rate of 0.5 MHz. Each single observation sequence requires that a full frameset be taken with a single CCD before switching to the next CCD for data acquisition. The focal-plane wiring is designed to prevent a single CCD failure from affecting more than half the focal plane; any single failure allows the two imagers on the other half of the focal plane to continue operating normally [6–8].

Figure 4 shows a diagram of a single SBV CCD imager [1]. The CCD layout was designed for three-side butting such that a $2 \times N$ focal-plane array could

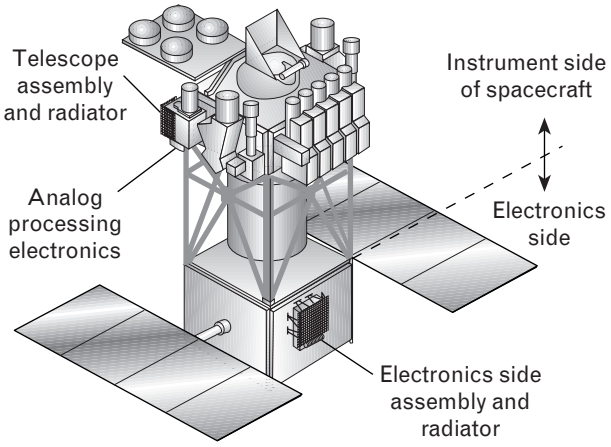

FIGURE 3. Relative location of the SBV sensor elements. The electronics of the SBV sensor and those of the other sensors were separated from the telescope and detector assemblies to prevent excessive thermal loading on the SPIRIT III infrared detectors. The SPIRIT III, an infrared imaging telescope, was the primary sensor on board the MSX satellite, and its focal planes had to be maintained at a temperature of 8°K. Reprinted from the *Johns Hopkins APL Technical Digest* by permission [1].

be fabricated. Each CCD has a 420 × 422-pixel imaging area and a 420 × 422-pixel storage area. The additional two lines in the image and storage areas allow for the possibility of some aluminum light-shield misalignment, and they reduce red diffusion effects of charge into the top of the storage area.

The CCD imagers are cooled actively. Waste heat is radiated to space by a radiator on (but thermally isolated from) the telescope body. The radiator is maintained at a minimum temperature of –43°C by survival heaters. A thermoelectric cooler is attached to the focal-plane Kovar tray through a flexible multilayer aluminum strap. The thermoelectric cooler is driven by an electronics servo system to maintain a maximum temperature of –40°C during operation. At this low temperature, dark current is on the order of eighteen electrons per pixel per second.

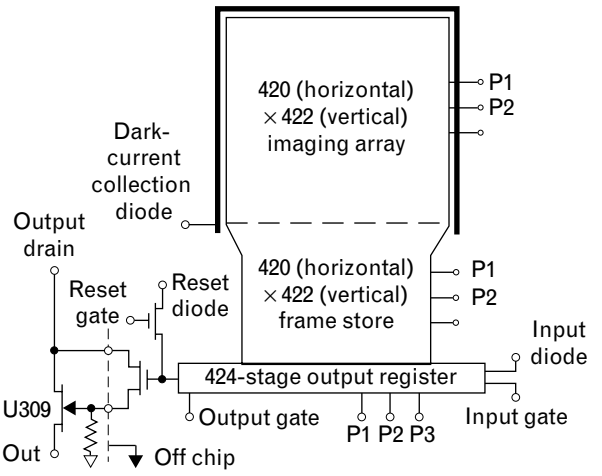

FIGURE 4. Block diagram of the CCD imager. Fabricated in the Solid State division at Lincoln Laboratory, each of the four CCD detectors in the SBV sensor is a 420 × 422-pixel, front-illuminated, frame-transfer imaging device, maintained on orbit at a temperature of –40°C by a thermoelectric cooler. Reprinted from the *Johns Hopkins APL Technical Digest* by permission [1].

CCD Camera

The camera selects the operating CCD, generates CCD focal-plane clocks and biases, coordinates timing with the other SBV elements, and provides a low-noise twelve-bit digitized readout. The camera uses a fully redundant, dual-channel architecture for fault tolerance, only one channel of which is powered at a time. The camera has two commandable gains and up to five different integration times. The gains are nominally set to provide six and twenty-five electrons per least significant bit of the twelve-bit analog-to-digital converters for full-scale responses of about 24,000 and 100,000 electrons, respectively.

Two integration times (0.4 and 1.6 sec) are used during space-surveillance operations, and three other integration times (0.625, 1.0, and 3.125 sec) are used for target-track and background-phenomena measurements, requiring the MSX tape recorder to operate. The camera can gate its output and synchronize to an external pulse, allowing accurate precise time tagging of space-surveillance integration times.

Signal Processor

The signal processor hardware can accept from two to sixteen data frames from the camera; each frame consists of about two megabits of information. Using this data, the signal processor automatically detects targets and reduces the data flow to a few kilobits per frame-set, effectively making a data compression ratio of greater than 1000:1. The signal processor has two redundant channels, each of which uses a Motorola DSP56001 digital signal processor operating at 20 MHz as its processing engine. The algorithmic core of the signal processor is centered around an assumed velocity filter that employs maximum-likelihood estimation for clutter rejection and automatic target detection. A one-bit binary implementation of this algorithm reduces the computational load while maintaining as much performance as possible from a full twelve-bit binary assumed velocity filter. The signal processor algorithm normally operates with the spacecraft stabilized in inertial space, with stars stationary, and with the images of moving objects forming streaks in the focal plane. This mode is referred to as sidereal track. The signal processor automatically detects these streaks and generates target reports consisting of position and velocity estimates in focal-plane coordinates. A target signature, using twelve-bit camera information, can also be included in the target report if commanded. The signal processor can also save a commandable number of the brightest stars' twelve-bit data for telemetering to the ground. The star data are used to refine the pointing knowledge of the SBV sensor.

The detection algorithm is run in two stages. While the camera is transmitting data, the signal processor has a real-time stage. Data are stored in three arrays—an average of all frames, the peak value of the frameset, and the second-highest peak value of the frameset. Frame number of occurrence is stored along with the values in the peak value and second-highest peak value arrays. When the data set is completed, the signal processor enters its second stage, in which stars are selected and the main part of the detection algorithm is run. Data from the second-highest value are used to estimate the variance of a pixel. After subtraction of the average frame data from the peak data, the result is divided by the variance estimate array. This new array has higher values for pixels that saw a changing scene during the frameset, corresponding to anything that had motion relative to the stars. The values are thresholded, which provides the single-bit array for the detection process.

Support Electronics

The support electronics comprise an experiment controller, a power subsystem, and a telemetry interface module. The experiment controller is based on a μDACS (micro-packaged data and control system) computer from SCI Inc., of Huntsville, Alabama. This controller is a Harris 80RH86 microprocessor-based computer with a high degree of fault tolerance and error correction. All control busses are triply redundant with majority logic, and the address and data busses have single-bit error-correction syndrome bits. The bus redundancy and error correction allows the μDACS to operate with no loss of speed, functionality, or capacity after the failure of any internal signal line. The experiment controller is used to read commands uplinked from the ground through the MSX spacecraft and to convert them to the set of commands to operate the SBV sensor. Under ground command, the experiment controller is used to configure all the other redundant electrical units of the SBV sensor by power and signal switching, and to provide health and status messages to the telemetry. Memory inside the experiment controller permits storage of many signal processor results, allowing the SBV sensor to gather and store observation results by using neither the MSX tape recorders nor contact with a ground station. When the spacecraft is over a ground receiving site, the MSX telemetry system relays the stored data to the ground.

The power subsystem was built for Lincoln Laboratory by Gulton Data Systems, Albuquerque, New Mexico. It provides conditioned, isolated secondary power for all units except the experiment controller, which has an internal power conditioner. It also switches primary and secondary power under experiment-controller control for fault recovery.

The telemetry interface module, designed and built at Lincoln Laboratory, is a first-in first-out unit capable of running up to the maximum instantaneous bit rate of 25 Mbits/sec. It is used to interleave the SBV telemetry into the MSX telemetry stream. The telemetry interface module interfaces to a redundant MSX telemetry system with a complete independent interface circuit assigned to each spacecraft system. The high bit rates used in the MSX telemetry system would have made a cross-strapping scheme large and power hungry, which was inconsistent with the weight and power budgets for the SBV sensor.

REFERENCES

1. D.C. Harrison and J.C. Chow, "The Space-Based Visible Sensor," *Johns Hopkins APL Tech. Dig.* **17** (2), 1996, pp. 226–236. Figures 2–4 in this appendix are reprinted from this earlier article in the *Johns Hopkins APL Technical Digest* by permission. These three images are ©The Johns Hopkins University Applied Physics Laboratory.
2. C.P. Dyjak and D.C. Harrison, "Space-Based Visible Surveillance Experiment," *SPIE* **1479,** 1991, pp. 42–56.
3. D.C. Harrison and J.C. Chow, "Space-Based Visible Sensor on MSX Satellite," *SPIE* **2217,** 1994, pp. 377–387.
4. D. Wang, L. Gardner, W. Wong, and P. Hadfield, "Space-Based Visible All-Reflective Stray Light Telescope," *SPIE* **1479,** 1991, pp. 57–70.
5. M.D. Morelli and S.E. Forman, "Prevention of Particulate Contamination from Fasteners on the Space-Based Visible Telescope," *SPIE* **1754,** 1992, pp. 249–260.
6. B.E. Burke, J.A. Gregory, R.W. Mountain, J.C.-M. Huang, M.J. Cooper, and V.S. Dolat, "High-Performance Visible/UV CCD Imagers for Space-Based Applications," *SPIE* **1693,** 1992, pp. 86–100.
7. B.E. Burke, R.W. Mountain, P.J. Daniels, and D.C. Harrison, "420 × 420 Charge-Coupled Device Imager and Four-Chip Hybrid Focal Plane," *Opt. Eng.* **26** (9), 1987, pp. 890–896.
8. B.E. Burke, R.W. Mountain, D.C. Harrison, M.W. Bautz, J.P. Doty, G.R. Ricker, and P.J. Daniels, "An Abuttable CCD Imager for Visible and X-Ray Focal Plane Arrays," *IEEE Trans. Electron Devices* **38** (5), 1991, pp. 1069–1076.

APPENDIX 2: CALIBRATION AND TESTING

THE PROCESS OF CALIBRATION and end-to-end system testing was instrumental to the success of the SBV sensor. The calibration effort resulted in a detailed understanding of the performance of the SBV sensor and allowed the conversion of SBV sensor observations into accurate measurements. The end-to-end testing established the confidence that the SBV flight hardware would function as expected after launch, and was key to the development of the ground-based command and data processing capability in the SPOCC.

Calibration

Most of the calibration efforts went into the telescope and focal plane. Measurements made early in the development process verified that the electronics had insignificant effects on system calibration compared with calibration-source stabilities and equipment-setup repeatability. An engineering model of the electronics was interchanged with the flight electronics with no detectable changes. Figure 1 shows a cutaway drawing of the telescope and a field-of-regard view in spacecraft coordinates [1]. The telescope has a distorted field of regard, a tradeoff made against focus quality and design time. The distortion requirement was driven by the signal processor; to maintain a high probability of detection any straight line in space projected onto the focal plane would have no more than 0.2-pixel deviation from a straight line over a 100-pixel length. Focus quality and radiometric calibration were also critical measurements.

Distortions were mapped by projecting a helium-neon laser spot sequentially to 256 positions per CCD imager and then calculating thirty-two coefficients (sixteen per axis) for a polynomial fit. Each CCD imager had its own set of coefficients. In all cases the errors were well below the 0.2-pixel data-analysis error budget.

Flat-field uniformity was measured by placing a large integrating sphere in front of the telescope aperture. Three separate flat-field functions were noted: (1) as predicted by the optical design, the steradiancy of pixels varied somewhat as a function of field position; (2) there was a slight misalignment of a light shield over the focal plane; and (3) the CCD imager had an inherent sensitivity pattern. Over the field of regard, the flat-field nonuniformity was about 12%, mostly due to the predictable steradiancy change. All effects were repeatable to better than 1%.

Radiometric calibration accuracy was defined as the residual errors after compensating for the stable flat-field patterns and reference radiometer accuracy. Data were taken with the same large integrating sphere used for flat-field measurements. Data errors

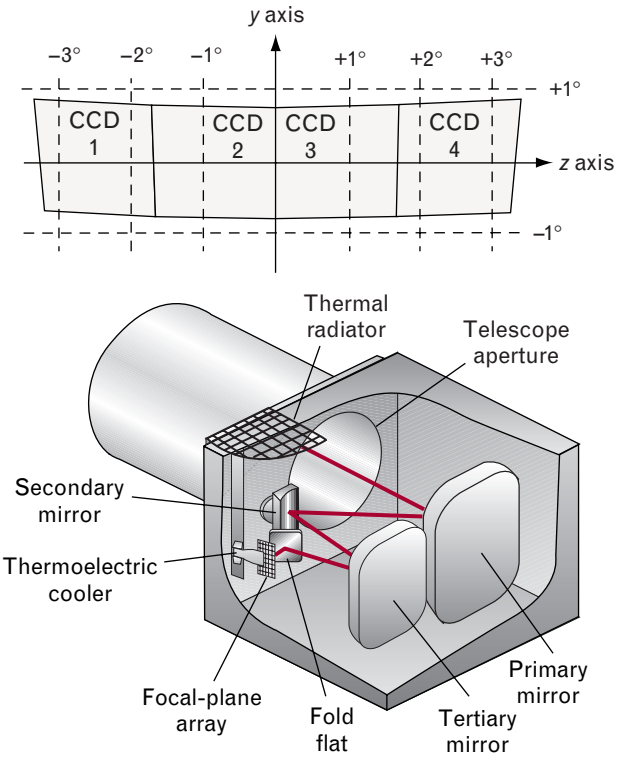

FIGURE 1. The SBV telescope and focal-plane projection of the four CCD imagers. Because of the off-axis design of the SBV sensor, a considerable amount of well-defined distortion exists within the images. This distortion is removed mathematically on the ground in the data-reduction processing pipeline. Reprinted from the *Johns Hopkins APL Technical Digest* by permission [1].

were dominated by equipment calibration accuracy, setup repeatability, and drift, rather than inherent sensor instabilities. The calibration variations had a repeatability of about 2.5% and are estimated to have absolute errors of less than 10%, which is well within the required 20%. Additional effort was not expended to refine the radiometric calibration process once the program requirements had been exceeded.

Dark current and noise tend to be related in CCD camera systems. At a focal-plane temperature of –40°C, the nominal operating temperature, the imagers had a dark current of eighteen electrons per second per pixel, well within the allowed limit of one hundred electrons per second. Noise, with the cover closed, measured to be 1.1 digital numbers root-mean squared (rms) at a 0.4-sec integration time, resulting in a noise of 6.9 electrons rms. Noise was measured both as a temporal variation of a single pixel and as an area average in a single frame. Both methods gave the same results. Focal-plane calibrations conducted prior to integration to the telescope showed that the SBV CCDs were capable of transferring charge packets as low as ten electrons with no apparent loss. The charge transfer remained unchanged down to operating temperatures of –55°C, where the dark current was less than two electrons per pixel. The focal planes were screened for pocket density (pockets are electron traps in the imager that cause a variety of temporal and spatial imaging distortions). There were no pockets noted greater than one hundred electrons on any imager, and none were detectable on CCD 3, the boresite imager.

The last calibration parameter was the bidirectional reflectance distribution function (BRDF), a measure of the scattering mechanisms inside the telescope. Figure 2 shows the BRDF measurement history of the telescope over nearly two years, where the sensitivity of the SBV sensor is plotted over time at two different tangent angles above a fully illuminated earth disk. The telescope was delivered to the vendor meeting its specification; the BRDF, however, seems to be slowly degrading with time, probably because of minor particle buildup on the mirrors. The sensitivity is calculated from measured BRDF data and plotted in Figure 2 as the minimum-diameter specular sphere detectable with a signal-to-noise ratio of six at altitudes of both 100 km and 350 km above the earth tangent point. Smaller diameters indicate better detection sensitivity, which corresponds to better rejection of the sunlight reflected from the earth. The rolloff is slower than was expected, allowing the SBV sensor to meet its performance requirements, even with some additional future contamination. The telescope has not been cleaned since delivery; we believe that the good level of cleanliness is due to strict adherence to contamination control procedures and to design decisions made with contamination control in mind. In fact, the contamination control was so successful that the SBV sensor arrived on orbit with the same BRDF as measured on the ground prior to launch. This lack of contamination is a significant achievement, since the launch vibrations could have easily redistributed any contaminants in the telescope to the mirrors.

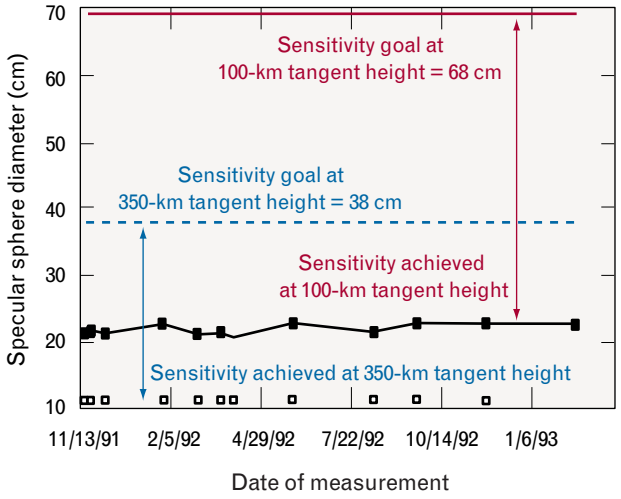

FIGURE 2. Measurement history of the bidirectional reflectance distribution function (BRDF). The BRDF, a measure of scattering mechanisms within the telescope, is a key metric in the determination of the sensitivity of the SBV sensor. The red line indicates the original design goal of detecting a 68-cm sphere at a tangent height of 100 km, while the dashed blue line represents the goal of detecting a 38-cm sphere at a tangent height of 350 km. The actual performance of the SBV sensor is indicated by the solid black squares for a 100-km height and by the open black squares for a 350-km height.

End-to-End Testing

With a system as complex as the SBV sensor, there is always the worry that a critical parameter has been

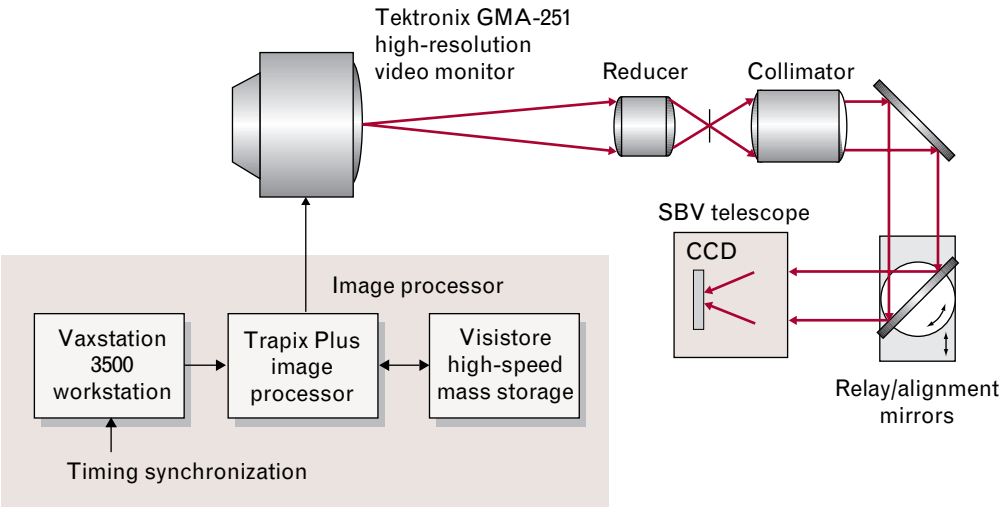

FIGURE 3. End-to-end test block diagram. The SBV sensor was designed, integrated, tested, and calibrated at Lincoln Laboratory, prior to its integration on the MSX satellite at the Johns Hopkins University Applied Physics Laboratory. Reprinted from the *Johns Hopkins APL Technical Digest* by permission [1].

missed and the SBV sensor will not work properly on orbit. Ideally, prior to launch, the sensor should be taken to an observatory where it could operate by looking at real scenes containing clutter (stars) and moving objects (satellites). However, the risk of contaminating the telescope forced us to reject this idea. To simulate a real observation, Lincoln Laboratory assembled an optical scene generator to project images into the telescope. Figure 3 shows a block diagram of the end-to-end test setup [1].

A series of complex framesets were generated by a VAX workstation and loaded into a Tektronix high-resolution video monitor. These scenes contained stationary objects simulating stars and moving objects simulating satellites. The scenes simulated variable star brightnesses and several different satellite motions. The monitor images were projected through a collimator into the SBV telescope. After alignment to a CCD, the framesets were synchronized to the SBV camera's timing by using test port signals. The resulting images were collected by the camera and sent to the signal processor. The results were then checked against predictions.

The flight hardware detected all objects and sent correct message types to the ground data-analysis system. Just one problem was found; the metric positions of the simulated stars were in error. This problem was traced to distortions in the scene generator, both static and dynamic. The test was repeated for the remaining three CCDs in the SBV focal plane, and no other problems were found.

The data acquired during the end-to-end tests were input to the SPOCC data-reduction process to verify proper function and to validate that the expected accuracy could be achieved. With calibration completed, the remaining tasks were to integrate the SBV sensor into the MSX spacecraft at the Applied Physics Laboratory at Johns Hopkins University, and run through the spacecraft-level testing. The electronics were integrated successfully in March 1993 and the telescope was integrated successfully in May 1994.

REFERENCES

1. D.C. Harrison and J.C. Chow, "The Space-Based Visible Sensor," *Johns Hopkins APL Tech. Dig.* **17** (2), 1996, pp. 226–236. Figures 1 and 3 in this appendix are reprinted from this earlier article in the *Johns Hopkins APL Technical Digest* by permission. These two images are ©The Johns Hopkins University Applied Physics Laboratory.

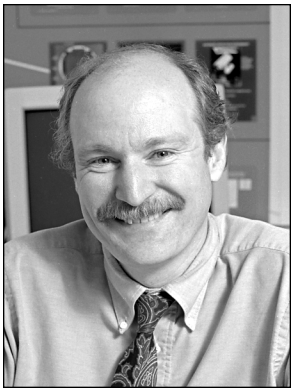

GRANT H. STOKES
is the assistant division leader of the Aerospace division, where he specializes in analysis, design, and operations of space-surveillance systems, including the Space-Based Visible (SBV) and LINEAR programs. The SBV system provides the first space-based space-surveillance capability to Air Force Space Command in Colorado Springs, Colorado. The LINEAR program utilizes space-surveillance technology developed for the U.S. Air Force to search for near-earth asteroids. Before coming to Lincoln Laboratory in 1989, Grant worked as a senior scientist and operations manager at Geo-Centers Inc., a contracting company specializing in fiber-optic sensors. Previously, he performed nondestructive testing of laser fusion targets at Los Alamos National Laboratory in New Mexico, and developed fiber-optic data-acquisition systems and provided field support for underground nuclear tests in Nevada. He holds a B.A. degree in physics from Colorado College, and M.A. and Ph.D. degrees in physics from Princeton University.

CURT VON BRAUN
is a staff member in the Surveillance Techniques group, where he conducts research in space surveillance, sensor calibration, and orbit determination and analysis. Before coming to Lincoln Laboratory in 1994, he was a researcher at the GeoForschungsZentrum (Earth Research Center) in Potsdam, Germany, and the Deutsches Geodaetisches Forschungsinstitut (German Geodetic Research Institute) in Munich, Germany. In both places he worked on orbital analysis of the Space Shuttle for the joint German/U.S. shuttle mission in 1993. He received a B.S. degree from Arizona State University, an M.S. degree from the University of Michigan, and a Ph.D. degree from the University of Texas at Austin, all in aerospace engineering. Currently he is the MSX Surveillance Principal Investigator and head of operations for the MSX/SBV Advanced Concept Technology Demonstration.

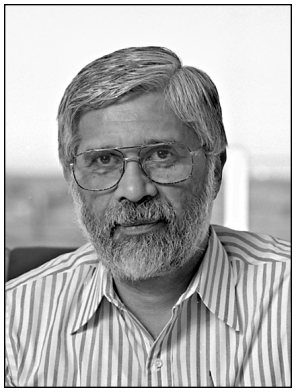

RAMASWAMY SRIDHARAN
is associate group leader in the Surveillance Techniques group and project leader at the Lincoln Laboratory Space-Surveillance Complex. The focus of his research is in space surveillance, including the detection and tracking of satellites with optical and radar systems. He received a B.E. degree in electrical engineering from the V.J.T. Institute, Bombay, India, and a Ph.D. degree in electrical engineering (applied space science) from Carnegie-Mellon University. Since joining Lincoln Laboratory in 1973, he has been involved in a variety of projects relating to space surveillance, including the Millstone Hill radar, the Haystack radar, ALTAIR, and the Space-Based Visible program. He is also progenitor of the Space Control Conference held every April at Lincoln Laboratory.

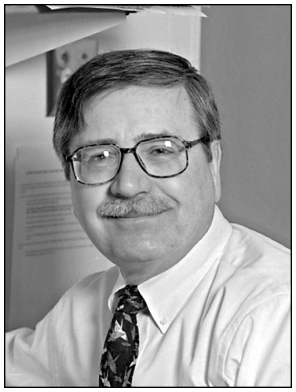

DAVID HARRISON
is a senior staff member in the Advanced Systems and Sensors group. He has devised electro-optical and other imaging systems for more than thirty years, concentrating on slow-scan applications of charge-coupled devices (CCD) during the last twenty-one years, including the last seventeen years at Lincoln Laboratory. He is the architect of many of Lincoln Laboratory's high-performance CCD focal-plane imagers, and he was the systems engineer for the SBV sensor. After receiving an S.B. degree in electrical engineering from MIT, he was the project engineer for the high-resolution X-ray imager, or HRI, that was successfully flown on both the Einstein High-Energy Astrophysics Observatory (HEAO-2) spacecraft and the West German Roentgen Satellite, or Rosat. The latest variant of his HRI design is installed on the Advanced X-ray Astrophysics Facility (AXAF) spacecraft, known as the Chandra Observatory, which is the last of the NASA great observatories. Over the course of his career he has provided varying levels of support for the Apollo Mission, Skylab, ANS, HEAO-1, HEAO-3, Spacelab-2, and the International Solar Polar Mission. He also served as the system engineer for the initial stages of NASA's Advanced Land Imager, to be flown on the Earth Orbiter 1 spacecraft. Currently, he is lead electrical engineer on the GeoLITE Lasercom Terminal project.

JAYANT SHARMA
is a staff member in the Surveillance Techniques group, where he works to extend the utilization of space-surveillance data. He has been extensively involved in SBV data processing and analysis. His other research interests include astrodynamics with an emphasis on orbit determination. Before joining Lincoln Laboratory in 1995 he worked at a small research company near Boston and at the Jet Propulsion Laboratory in Pasadena, California. Jayant received a B.S. degree and a Ph.D. degree in aerospace engineering from the University of Texas at Austin, and an S.M. degree in aeronautical and astronautical engineering from MIT.